Enhanced arecoline derivatives as muscarinic acetylcholine receptor M1 ligands for potential application as PET radiotracers

Marius Ozenil, Katharina Pacher, Theresa Balber, Chrysoula Vraka, Alexander Roller, Wolfgang Holzer, Helmut Spreitzer, Markus Mitterhauser, Wolfgang Wadsak, Marcus Hacker, Verena Pichler

PII: S0223-5234(20)30595-X

DOI: https://doi.org/10.1016/j.ejmech.2020.112623

Reference: EJMECH 112623

To appear in: *European Journal of Medicinal Chemistry*

Received Date: 28 May 2020

Revised Date: 17 June 2020

Accepted Date: 18 June 2020

Please cite this article as: M. Ozenil, K. Pacher, T. Balber, C. Vraka, A. Roller, W. Holzer, H. Spreitzer, M. Mitterhauser, W. Wadsak, M. Hacker, V. Pichler, Enhanced arecoline derivatives as muscarinic acetylcholine receptor M1 ligands for potential application as PET radiotracers, *European Journal of Medicinal Chemistry*, https://doi.org/10.1016/j.ejmech.2020.112623.

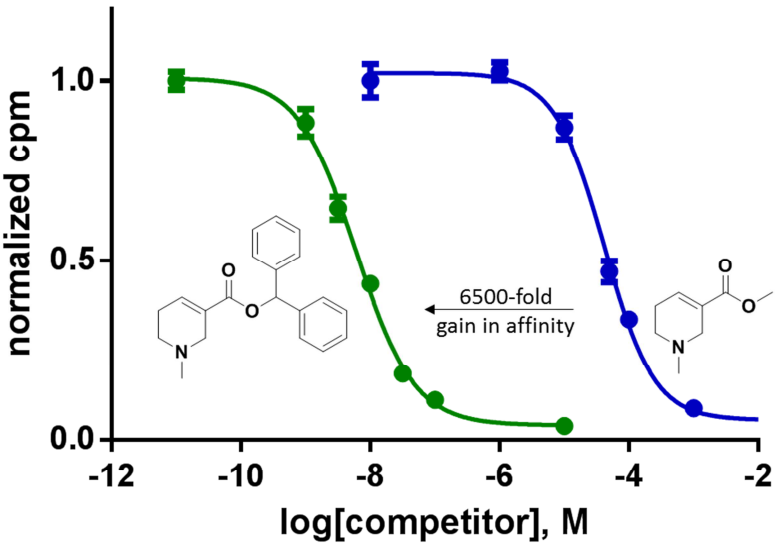

Enhanced arecoline derivatives as muscarinic acetylcholine receptor M1 ligands for potential application as PET radiotracers

Marius Ozenil,[1] Katharina Pacher,[1] Theresa Balber,[1,2] Chrysoula Vraka,[1] Alexander Roller,[3] Wolfgang Holzer,[4] Helmut Spreitzer,[4] Markus Mitterhauser,[1,2] Wolfgang Wadsak,[1,5] Marcus Hacker,[1] Verena Pichler[1,*]

[1] *Department of Biomedical Imaging and Image-guided Therapy, Division of Nuclear Medicine, Medical University of Vienna*

[2] *Ludwig Boltzmann Institute Applied Diagnostics, Vienna*

[3] *X-ray Structure Analysis Centre, Faculty of Chemistry, University of Vienna*

[4] *Department of Pharmaceutical Chemistry, Faculty of Life Sciences, University of Vienna*

[5] *CBmed GmbH - Center for Biomarker Research in Medicine, Graz*

*corresponding author

Abstract

Supported by their involvement in many neurodegenerative disorders, muscarinic acetylcholine receptors (mAChRs) are an interesting target for PET imaging. Nevertheless, no radiotracer is established in clinical routine. Within this work we aim to develop novel PET tracers based on the structure of arecoline. Fifteen novel arecoline derivatives were synthesized, characterized and tested for their affinity to the mAChRs M1-M5 and the conceivable off-target acetylcholinesterase. Five arecoline derivatives and arecoline were labeled with carbon-11 in good yields. Arecaidine diphenylmethyl ester (**3b**), arecaidine bis(4-fluorophenyl)methyl ester (**3c**) and arecaidine (4-bromophenyl)(4-fluorophenyl)methyl ester (**3e**) showed a tremendous gain in mAChR affinity compared to arecoline and a pronounced subtype selectivity for M1. Metabolic stability and serum protein binding of [^{11}C]**3b** and [^{11}C]**3c** were in line with properties of established brain tracers.

Nonspecific binding of [^{11}C]**3c** was prevalent in kinetic and endpoint experiment on living cells as well as in autoradiography on native mouse brain sections, which motivates us to decrease the lipophilicity of this substance class prior to *in vivo* experiments.

Keywords: muscarinic acetylcholine receptors, PET, carbon-11, neuroimaging

Introduction

Muscarinic acetylcholine receptors (mAChRs) are G-protein coupled receptors, which bind acetylcholine as endogenous ligand. Naming of the mAChRs is based on the additional activation by the fungal toxin muscarine. Their involvement in neurotransmission of the central nervous system as well as in the regulation of heart rate, muscle contraction and glandular secretion assigns mAChRs a pivotal role in physiology.[1] Conversely, alterations in mAChR signal transduction are involved in neurological disorders such as Schizophrenia, Alzheimer's or Parkinson's disease.[2] mAChRs are divided into five subtypes (M1-M5), all of which are expressed in the human brain. M1, M4 and M5 are expressed only in certain brain areas, whereas M2 and M3 are abundant throughout the brain.[3] The subtypes are classified by their activation of G proteins from the $G_{q/11}$ (M1, M3 and M5) or $G_{i/o}$ family (M2 and M4).[1] Comparison of the crystal structures of M1-M4 proteins showed high similarity, which leads to difficulties in the development of subtype selective mAChR ligands.[4] A closer relation of M1 to M4[5] was found compared to the structural relation of M1 to M3, which potentially explains that the clinically relevant antagonist pirenzepine displays a higher affinity to M1 and M4 than M2 and M3.[6] The neurotransmitter acetylcholine binds to the orthosteric binding site, which is highly conserved and sterically demanding. As a consequence, a huge amount of ligands described in literature for mAChR are positive allosteric modulators (PAMs).[7] However, most of them suffer from limited affinity.[1]

The naturally occurring alkaloid arecoline exhibits orthosteric partial agonist properties toward mAChRs and is found in the betel nut. Its stimulating effects in the central nervous system underline its ability to cross the blood brain barrier.[8] Although arecoline is also known to have activity on selected nicotinic acetylcholine receptors[8], derivatization with typical muscarinic moieties as applied within this work is strongly expected to deliver muscarinic selectivity. The inhibitor constants (K_i) of arecoline toward mAChRs were determined to be in the range of 15-77 µM,[9] which is certainly insufficient for mAChRs positron emission tomography (PET) imaging. However, arecoline might act as a suitable lead structure for the development of high affinity mAChR ligands.[10] A

typical pharmacophore in the orthosteric mAChR M1 binding motif displays a 'cationic head' which interacts with the Asp105A residue.[11] In arecoline this feature is represented by the protonated tertiary amine. Derivatives of arecoline should not contain bulky residues on the amine in order to maintain the critical cationic head. In fact, studies on previously synthesized arecoline derivatives confirmed that replacement of the *N*-methyl group of arecoline resulted in reduction or a complete loss of agonistic activity.[12] Instead it appears feasible to use the *N*-methyl position unchanged, leaving the *O*-methyl position open for chemical derivatization. The *O*-methyl position is moreover the attack point for esterases leading to arecaidine as metabolite.[13] Moreover, the introduction of carbon-11 at the *N*-methyl position does not alter the investigated structure leading to similar behaviour as the unlabeled preclinically investigated compound and open up the possibility for application in PET. PET is a non-invasive imaging modality and can be used to study receptor distribution and occupancy in brain or the peripheral nervous system. Considering the mAChR density in brain, it can be estimated that the affinity constant for a mAChR tracer should be around 3-50 nM for *in vivo* imaging.[14,15] Numerous animal and human imaging studies of mAChRs have been undertaken in healthy and diseased brain. Till now, no protocol has been established in clinical routine. Considering that acetylcholine was the first neurotransmitter to be discovered, even further presses the question why mAChR-imaging has not yet found its way into clinics. On the one hand, this can be attributed to the current lack of impact on clinical decisions derived from information obtained from mAChRs imaging.[10] On the other hand, the ongoing research effort put on novel radiotracers for mAChRs (Figure 1) emphasizes that imaging properties of current radiotracers are still to be improved.

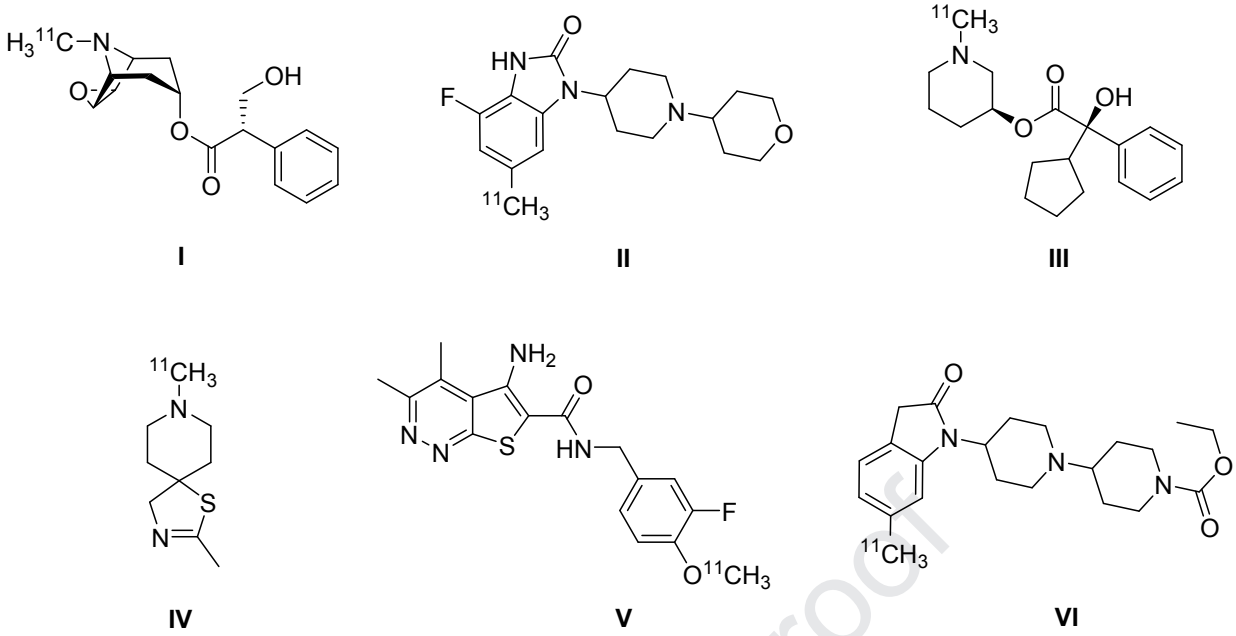

Figure 1: Structures of carbon-11 radioligands investigated as mAChR PET tracers.

In the early days of mAChR tracer development, ligands with excessive affinity (*e.g.* [^{11}C]scopolamine[16] (**I**), [^{11}C]benztropine[17]) heavily caused flow-dependent accumulation. More recent mAChR tracer developments, [^{11}C]GSK1034702[18] (**II**) and (S,R)-1-methylpiperidin-3-yl)2-cyclopentyl-2-hydroxy-2-phenylacetate[19] (**III**), suffer from low specific *in vivo* binding and the agonist [^{11}C]AF150(S)[20] (**IV**) was deemed challenging for *in vivo* applications because of its rapid metabolism and limited binding affinity. Furthermore, one of the main challenges in current mAChR tracer development remains subtype selectivity[21], since for the majority of mAChR ligands subtype selectivity and affinity have been contradictory properties.[1] The high affinity M4 PAM [^{11}C]VU0467485 (**V**) and two of its congeners overcome this discrepancy, yet limited specific binding and insufficient BBB permeability stopped their further development.[22] [^{11}C]LSN3172176 (**VI**) can currently be considered as the most promising candidate for clinical mAChR M1 imaging and was just advanced to human studies for further evaluation.[23] A BBB penetrant selective mAChR M1 PET tracer would not only allow to investigate the molecular pathology of brain diseases, but also facilitate the discovery of drugs for therapeutic applications.[23]

In this study, we aim to significantly enhance the potency of arecoline derivatives by synthesis of a set of orthosteric compounds targeting the mAChR M1. We investigated their physico-chemical behaviour and affinity toward all five muscarinic acetylcholine receptors. The most successful candidates of this preclinical screening showed affinity in the low nanomolar range, and were radiolabeled with carbon-11 for further pharmacological characterization toward radiotracer development for PET.

Results and Discussion

Synthesis of arecoline-based low molecular weight compounds

Starting from arecaidine (1-methyl-3,6-dihydro-2*H*-pyridine-5-carboxylic acid) and 4-methylmorpholine-2-carbonitrile a set of fifteen compounds was synthesized and six precursors required for potential radiolabeling with carbon-11 were prepared from *N*-protected guvacine. Figure 2 and Figure 3 outline the synthetic routes for arecoline derivatives (**1**-**3**). **1a** was prepared by methylation of *N*-Fmoc guvacine in presence of Na_2CO_3. Esters **1b**-**c** were prepared by reacting *N*-Fmoc guvacine with alcohols activated as trichloroacetimidate. **1j** was prepared *via* the acid chloride route. Activation of *N*-protected or unprotected arecaidine with *N*,*N'*-dicyclohexylcarbodiimide and subsequent spontaneous migration of the acyl residue gave the *N*-substituted urea derivatives **1k** and **3k**. Fmoc deprotection by diethylamine afforded compounds **2a**-**c** and **2j**-**k**. Precursor **2i** was obtained by Boc removal in presence of trifluoroacetic acid. **1i** and **3b**-**j** were synthesized *via* carbonyldiimidazol-mediated coupling. **3l**-**m** were prepared by alkylation with an α-chloro amide. Preparative chromatography using an alpha-1-acid glycoprotein stationary phase allowed for chiral resolution of **3e**.

The protected precursor compounds (**1**) were synthesized in good to excellent yields, whereas the synthesis of the non-radioactive reference compounds (**3**) was more demanding leading to only moderate yields. This difference in yields can be explained by two factors, resulting from the

zwitterionic characteristics of arecaidine compared to *N*-Fmoc guvacine. Firstly, the limited solubility of arecaidine in most organic solvents necessitated DMF-compatible esterification procedures. Secondly, arecaidine's interionic interactions can reduce the access of the activating reagent to the carboxylic group.

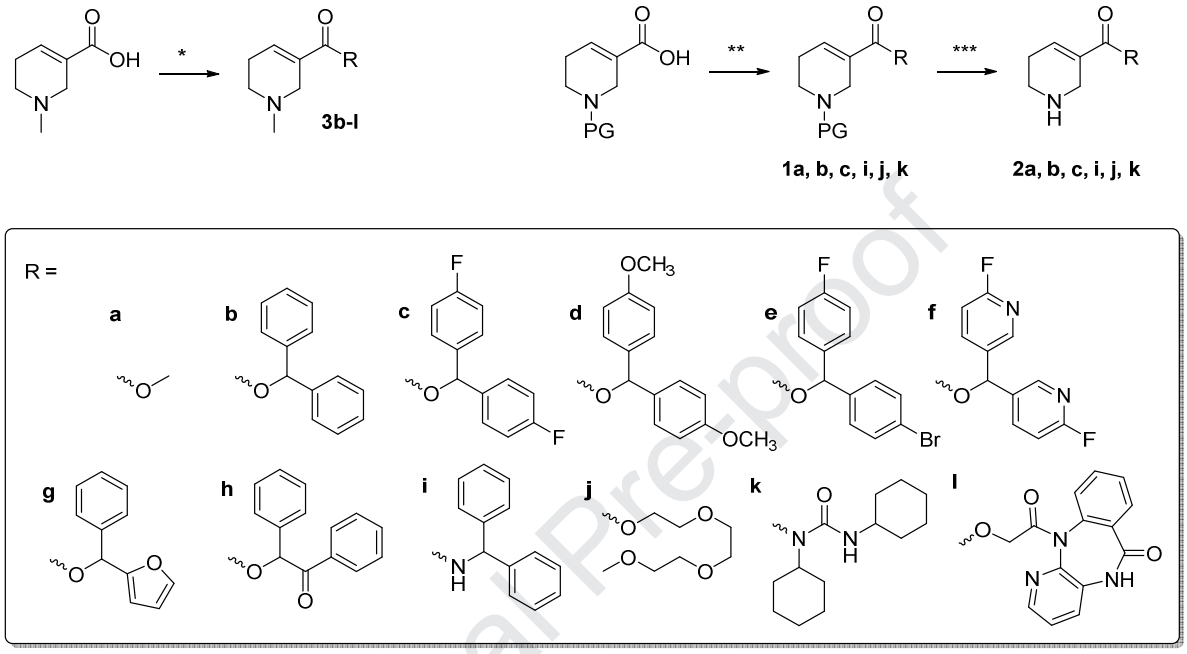

*Figure 2: Synthesis overview of arecoline derivatives (**3b**-**l**) and their N-desmethyl congeners (**2a**,**b**,**c**,**i**,**j**,**k**).* **3b**-**g**: 1. CDI, DMF 2. Na^+R^-, 3-25 %; **3h**-**j**: 1. CDI, DMF, 2. RH, 3-18 %; **3k**: DCC, DMF, 69 %; **3l**: 1. NaH in DMF, 2. NaI, 11-(chloroacetyl)-5,11-dihydro-6H-pyrido[2,3-b][1,4]benzodiazepin-6-one, 13 %. ** **1a**: PG = Fmoc, Na_2CO_3, CH_3I, DMF, 96 %; **1b**-**c**: PG = Fmoc, $RC(=NH)CCl_3$, DCM, 87-93 %; **1i**: PG = Boc, CDI, DMF, 2. RH, 12 %; **1j**: PG = Fmoc, 1. $SOCl_2$, 2. RH, 93 %; **1k**: PG = Fmoc, DCC, DMF, 48 %. *** **2a**,**b**,**c**,**j**,**k**: DEA, ACN, 63-93 %; **2i**: TFA, DCM, 79 %.*

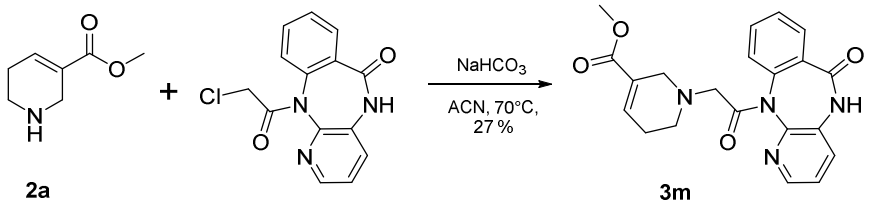

*Figure 3: Synthesis of the arecoline derivative **3m** by nucleophilic substitution.*

Derivatives of 4-methylmorpholine-2-carboxylic acid (**6**-**7**) were prepared as congeners with decreased lipophilicity compared to **3b** and **3i** (Figure 4). **6** was prepared by Ritter reaction in formic acid[24] from **4**. **8** was prepared by Grignard reaction with benzylmagnesium bromide from **4**.

Carbonyldiimidazol-mediated coupling of **5** with sodium diphenylmethanolate afforded **7**. Surprisingly, compounds **4** and **5** were not literature reported. Synthesis of **4** could be realized by addition of *N*-methylethanolamine to 2-chloro acrylonitrile and subsequent base cyclization, using an adopted procedure of Kopach *et al*.[25] Acidic hydrolysis of the nitrile **4** afforded compound **5**.

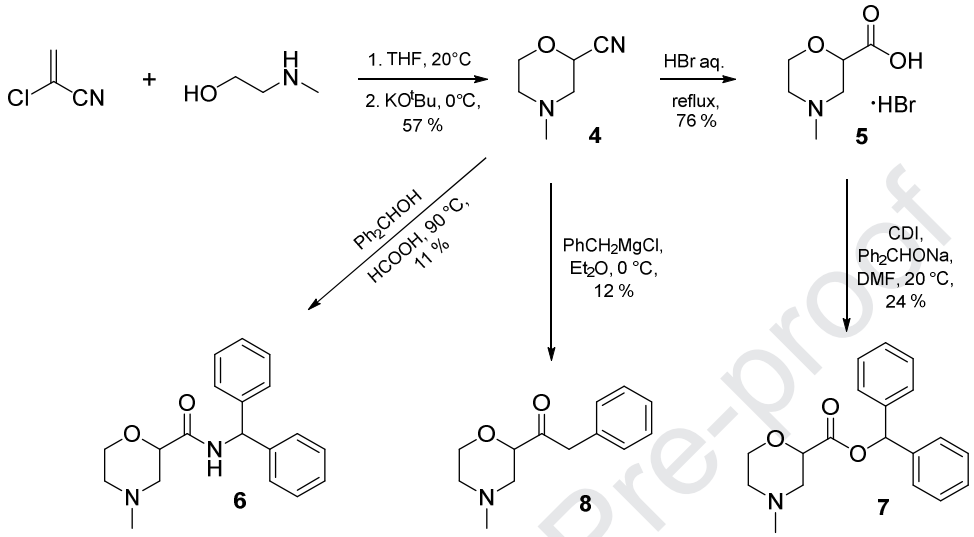

*Figure 4: Synthesis of 4-methylmorpholine-2-carbonitrile (**4**) and its related carboxylic acid (**5**). **4** and **5** were used for the synthesis of potential mAChR ligands **6**-**8**.*

Precursors (**2**) and non-radioactive reference compounds (**3, 6**-**8**) were fully characterized by 2D-NMR spectroscopy, HRMS and UV-HPLC. Regarding benzhydryl derived compounds, the shift and multiplicity of the benzylic proton signal is influenced by the type of the neighboring element and hence the type of carbonyl compound. Esters (**3b**-**g**, **7**) show a singlet at 6.86-7.00 ppm, whereas the amides **3i** and **6** exhibited a high field shifted signal at 6.28 ppm and 6.25 ppm respectively. Furthermore, the type of carbonyl compound influences the shielding of the respective vinylic proton of the arecaidine backbone. For the ester derivatives (**3b**-**h**, **3j**, **3l**) a multiplet at 6.87-7.32 ppm was observed, compared to a high field shifted mutliplet at 6.15-6.56 ppm for the amide derivatives (**3i**, **k**). In HRMS measurements all analyzed compounds could be ionized in positive mode yielding $[M+H]^+$ and/or $[M+Na]^+$ cations of expected masses.

Compound **3k** and **5** were isolated as monocrystals and analyzed by X-ray single crystal diffraction analysis. The compounds crystalized in an orthorhombic crystal system (space group Pna21) and in a monoclinic crystal system (space group P21/n), respectively. A detailed description is shown in the Supporting Information.

Subtype selectivity analysis toward muscarinic acetylcholine receptors

Inhibition constants (K_i) against mAChR subtypes of arecoline, **3b**-**m** and **6**-**8** were determined with a competitive radioligand binding assay applying the common mAChR ligand *N*-methyl-[^{3}H]scopolamine ([^{3}H]NMS). Arecoline, **3d**, **3j**-**m** and **8** feature inhibition constants in the micromolar range or higher against all mAChR subtypes, whereas **3b**, **3c, 3e-i**, **6** and **7** show a drastically increased affinity with values in the submicromolar to low nanomolar range (Table 1).

Table 1: Inhibition constants (K_i) given in nM, n≥3, determined by [^{3}H]NMS competition binding.

	M1	M2	M3	M4	M5
3a	20,300±2,400	3,800±890	16,700±5,900	4,700±410	7,000±570
3b	3.1±0.5	110±39	56±22	16±4	14±1
3c	5.0±1.6	710±110	77±28	19±5	32±5
3d	>4,700	>4,500	>2,200	>3,300	>2,600
(-)-**3e**	15.6±2.1	560±110	56±10	64±11	42±23
(+)-**3e**	7.8±1.7	670±70	52±6	42±2	27±5
3f	850±240	1480±40	690±170	720±420	690±70
3h	270±130	3300±500	1240±210	1200±500	800±190
3i	153±60	>4,500	1,500±290	400±74	580±130
3j	148,000±35,000	>4,500	>2,200	>3,300	>2,600
3k	204,000±53,000	>4,500	>2,200	>3,300	>2,600

3l	>4,700	>4,500	>2,200	>3,300	>2,600
3m	>4,700	>4,500	>2,200	>3,300	>2,600
6	610±50	>4,500	>2,200	>3,300	>2,600
7	710±90	>4,500	>2,200	>3,300	>2,600
8	>4,700	>4,500	>2,200	>3,300	>2,600

No specific competitive binding could be observed on membranes prepared from wild type CHO cells (negative control), proving the high specificity of these ligands in the competitive radioligand binding assay. The determined inhibition constants for arecoline (**3a**) match well with previously reported data.[9]

3l-**m** are conjugates of the arecoline backbone with the clinically applied M1-selective antagonist pirenzepine and were designed to promote subtype M1 selectivity. However, their low affinity excluded them from further development. Exchange of the *O*-methyl group of arecoline with a diphenylmethyl (**3b**), bis(4-fluorophenyl)methyl (**3c**) or (4-bromophenyl)(4-fluorophenyl)methyl (**3e**) moiety led to a tremendous increase of affinity toward all subtypes to levels suitable for PET tracers. Structures with fluorine substituents were investigated to enable potential use of fluorine-18 for radiolabeling. The affinity dropped strongly when arecaidine was substituted with 4-methylmorpholine-2-carboxylic acid (**6**, **7**). Enantiomers of **3e** show a distinct affinity profile, with a twofold difference in M1 affinity being the most notable difference (p = .007). Interestingly, **3b**, **3c** and **3e** show a preference for subtype M1, whereas arecoline (**3a**) shows a higher affinity for subtype M2 compared to M1. The derivatization of arecoline with diphenylmethyl moieties affected the subtype selectivity to such an extent that also in the overall subtype selectivity profile the difference in affinity is the highest between M1 and M2 for **3b** (35-fold), **3c** (140-fold), (-)-**3e** (36-fold) and (+)-**3e** (86-fold). From a thermodynamical perspective, the similar target densities of the subtypes in human brain[26] paired with the strong subtype selectivity for M1 over M2 should lead to an equally strong subtype selectivity in *in vivo* imaging. In **3b** and **3c** the subtype selectivity of M1 over M3-M5 is less

pronounced (between 2.7-fold and 18-fold), which might appear insufficient for subtype-selective *in vivo* imaging. However, [^{18}F]FP-TZTP, which is a known *in vivo* M2 selective tracer, features only 3.4-fold selectivity of the M1 over the M2 receptor *in vitro*.[27] Ravasi *et al.*[28] proposed, that *in vivo* M2 selectivity of [^{18}F]FP-TZTP is caused by the slower k_{off} from M2 compared to the other subtypes. This highlights the importance of ligand-receptor kinetics for mAChR tracer development and motivated us to study the *in vitro* kinetics of [^{11}C]**3c** (see section Interactions of [^{11}C]**3c** with CHO-M1 cells).

Specificity analysis of competing electric eel acetylcholinesterase (EeAChE) affinity and metabolism

Compounds **3a**-**m** and **6**-**8** could unintentionally act as ligand or substrate for AChE (acetylcholinesterase), which would cause specificity problems. AChE is a certainly conceivable off-target in the development of orthosteric ligands for mAChRs and especially of interest for arecoline-derived compounds when considering the structural similarity to the known AChE-inhibitors neostigmine and pyridostigmine.[29] Inhibition constants (K_i) against EeAChE (acetylcholinesterase from *Electrophorus electricus*) of **3a**-**m** and **6**-**8** and tacrine as positive control were determined by Ellman's assay. The obtained K_i of the positive control tacrine was 30 ± 10 nM, which corresponds well to the range of literature reported values[30] (for graphs see Supporting Information, Figure S7). For **3a**-**m** and **6**-**8** no inhibition compared to the blank could be perceived in the c_{ATI}/(sec/OD) diagram at the highest concentration tested (16.5 µM). Graphs are shown in the Supporting Information, Figure S6. Furthermore, a two-way ANOVA followed by a Dunnett's multiple comparisons test revealed that the slopes are not significantly different ($\alpha > 0.05$), which allows to conclude that the K_i against EeAChE of **3a**-**m** and **6**-**8** is higher than 16.5 µM.

Interestingly, no significant EeAChE metabolism could be observed for arecoline derivatives **3a**-**m** and **6**-**8** under these conditions, not even after 60 min of incubation ($\alpha > 0.05$). Overall, it was ruled out that **3a**-**m** and **6**-**8** are EeAChE substrates under the used assay conditions. Additionally, **3a**-**m** and **6**-**8** did not show any EeAChE inhibitory effects at concentrations up to 25 µM.

Concluding, the investigated set of mAChR ligands exhibits high specificity against the target of choice as they were neither inhibitors nor substrates to the off-target EeAChE.

HPLC-log$P_{ow}^{pH7.4}$ determination and structure-activity relationship

Although the predictive factor of HPLC-log$P_{ow}^{pH7.4}$ for prediction of blood brain barrier penetration is critically discussed in literature,[31–33] still this value is broadly determined in drug development. The HPLC-log$P_{ow}^{pH7.4}$ as a measure for the affinity of compounds to a lipophilic stationary phase allows estimation of nonspecific binding in fatty tissue, other lipophilic tissues or plasma protein binding and was therefore analyzed.

The HPLC-log$P_{ow}^{pH7.4}$ value was determined chromatographically and tPSA was calculated (Table 2). All target compounds (**3a**-**m** and **6**-**8**) exhibited HPLC-logP values in the range of established BBB permeable brain tracers[31] and **3a**-**k** and **6**-**8** exhibit a tPSA (total polar surface area) < 60 Å^2, supporting BBB penetration.[34]

Table 2: Overview of substance parameters. tPSA was calculated using ChemBioDraw 13.0.2.3021.

	tPSA [Å^2]*	HPLC-log$P_{ow}^{pH7.4}$
3a	29.54	-1.62±0.62
3b	29.54	3.32±0.04
3c	29.54	3.62±0.08
3d	48.00	3.07±0.04
3e	29.54	4.12±0.15
3f	54.26	1.91±0.17
3g	38.77	3.66±0.08
3h	46.61	2.94±0.05
3i	32.34	2.25±0.12
3j	57.23	-0.70±0.54

3k	52.65	2.24±0.13
3l	91.31	0.57±0.37
3m	91.31	0.96±0.31
6	41.57	2.30±0.12
7	38.77	2.79±0.05
8	29.54	1.00±0.30

222

223 For identification of the most promising compounds in terms of subtype selectivity independent from
224 the absolute value, the ratio values of the K_i of M4/M1 was correlated with the ones for M3/M1.
225 Three main groups could be recognized showing low subtype selectivity (Figure 5A, blue),
226 intermediate preference for M1 (Figure 6A, red) and high preference for M1 subtype (Figure 5A,
227 green). The three compounds with the highest preference for the M1 subtype were as follows in
228 increasing order: **3i** < **3c** < **3b**. Obviously, the diphenylmethyl moiety was crucial to achieve highly
229 improved subtype selectivity against the mAChR-M1 subtype compared to arecoline. Notable is also
230 the enantiomeric selectivity of (+)-**3e** over (-)-**3e** for mAChR-M1 giving the opportunity to fine-tune
231 the affinities *via* stereochemistry.

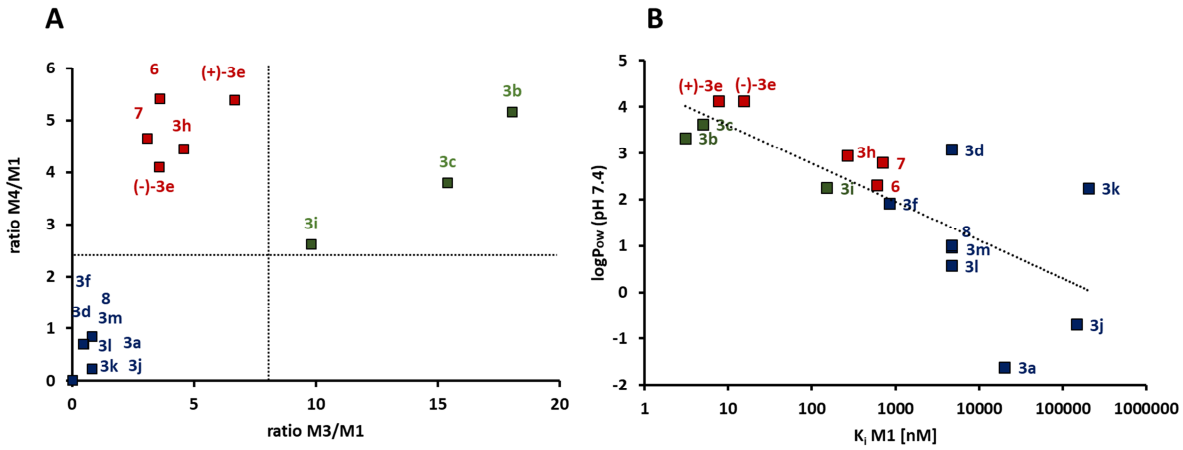

232

233 *Figure 5: (A)* ***Evaluation of the subtype selectivity by comparison of the ratio values of M4/M1 and M3/M1****. The analysis*
234 *identified a group of compounds with low subtype selectivity (blue), compounds with intermediate (red) and high preference*

for M1 (green). (B) ***Correlation of the pK_i toward M1 and the HPLC-$logP_{ow}$ (pH 7.4)****. A logarithmic trend was observed showing that higher lipophilicity leads to higher affinities.*

Correlation of the pK_i toward M1 and the $logP_{ow}^{pH7.4}$ values showed a logarithmic trend of affinity and lipophilicity (R^2 = 0,56). However, as the K_i of compounds **3d**, **3l**, **3m** and **8** toward M1 was higher than the concentration range of the experiment, only a trend analysis was possible. Especially, the analysis of the enantiomers (+)-**3e** and (-)-**3e** exemplarily shows, that an increase in affinity is possible without an alteration in lipophilicity and underlines the importance of enantiomeric selectivity for the binding to mAChR M1.

Overall, the most promising compounds in terms of subtype selectivity, absolute affinity against mAChR M1 and tPSA were **3b** and **3c**, which were further evaluated for radiolabeling with carbon-11. The isostere **3i** was additionally used for comparison purposes in metabolic studies.

Docking studies

Docking of protonated **3c** in the active center of mAChR M1 (PDB: 5CXV)[5] supports that it adopts a similar binding pose compared to tiotropium (Figure 6A).

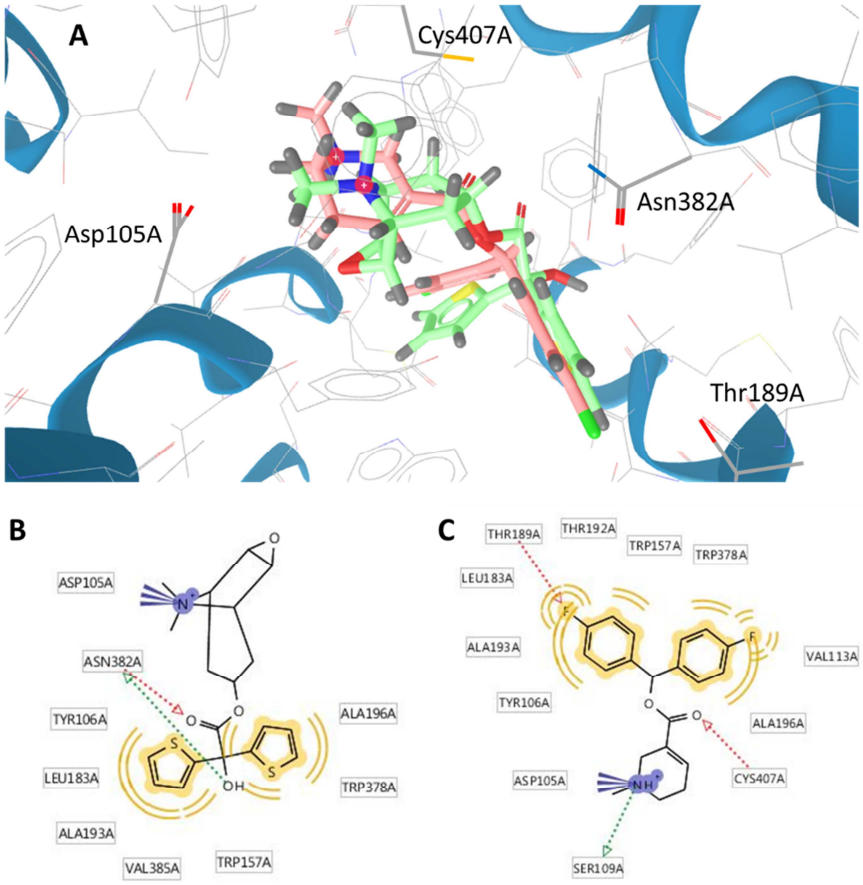

*Figure 6: A: Lowest binding energy docking poses of **3c** (salmon, -20.0 kcal/mol) and tiotropium (light green, -22.4 kcal/mol) in the orthosteric binding site of human M1 mAChR. Ser109A is covered by the docked ligands. B,C: Pharmacophore-derived interactions of tiotropium (B) and **3c** (C) with the binding pocket environment calculated and visualized with LigandScout.*

In this pose tiotropium as well as protonated **3c** feature electrostatic interaction of the quaternary ammonium cation with ASP105A and hydrophobic interactions of the aromatics to several apolar amino acid side chains. In the docked binding pose of tiotropium ASN382A acts as hydrogen bond donor and acceptor for the hydroxyl and carbonyl moiety, whereas in protonated **3c** the carbonyl acts as hydrogen bond acceptor for CYS407A. Additionally, protonated **3c** features hydrogen bonds to SER109A and THR189A (Figure 6C). Hydrogen bonds to organic fluorine have low binding energies, yet they are known to affect chemical behavior[35] and can hence potentially influence ligand binding.

Furthermore, we performed molecular docking of protonated **3b** and **3i** in order to get a molecular insight into the reason for the approx. 50-fold higher mAChR M1 binding affinity of **3b**.

Unexpectedly, in these docking experiments **3i** (lowest estimated binding energy: -20.3 kcal/mol; lowest binding affinity score: -31.4) performed even slightly better than **3b** (-20.2 kcal/mol; -26.9). Consequently, we assume that the experimentally observed loss of affinity of **3i** compared to **3b** is not based on the lack of a suitable conformer inside the binding pocket caused by the more rigid amide bond, but rather results from reduced flexibility during its way to the active center. Furthermore, also electronical differences of the neighboring moieties between **3b** and **3i**, as observed by NMR spectroscopy, could affect the capability of the ligands to reach the binding pocket.

Radiolabeling of the most promising compounds with carbon-11

The most promising compounds **3b** and **3c** regarding subtype selectivity, receptor specificity and physico-chemical parameters were chosen for radiolabeling. The radiolabelling of **3i** was performed for the analysis of metabolites obtained by liver microsomes. All other compounds were radiolabeled to show the substrate scope of the chosen reaction conditions. First small scale reaction were performed to investigate the optimal labeling conditions. Subsequently, fully-automated radiosyntheses were set up to study metabolism, plasma protein binding and cell binding.

Small scale reactions of compounds **2a**, **2b** and **2j** with [^{11}C]CH_3I yielded [^{11}C]**3a**, [^{11}C]**3b** and [^{11}C]**3j** (Figure 7) in good yields in both solvents, ACN (Table 3) and DMSO (Table 4) as determined by RP-HPLC without further purification. When using ACN, radiochemical yields[36] significantly increased with reaction time and temperature. In DMSO, labeling was almost quantitative at both tested reaction times and temperatures. Thus, DMSO at 20 °C for 2 min was initially chosen for implementation of the automated radiosynthesis.

*Table 3: Non-isolated radiochemical yields [%] in ACN as determined by radio-HPLC (ND = not determined, n = 1). ACN was not investigated as solvent for labeling of [^{11}C]**3j**, because an almost quantitative non-isolated radiochemical yield was observed using DMSO (Table 4).*

	[^{11}C]**3a**		[^{11}C]**3b**		[^{11}C]**3j**	
	20 °C	70 °C	20 °C	70 °C	20 °C	70 °C
2 min	23	55	37	58	ND	ND
5 min	33	81	45	68	ND	ND

Table 4: Non-isolated radiochemical yields [%] in DMSO as determined by radio-HPLC (n = 1).

	[^{11}C]**3a**		[^{11}C]**3b**		[^{11}C]**3j**	
	20 °C	120 °C	20 °C	120 °C	20 °C	120 °C
2 min	92	91	79	87	98	95
5 min	93	91	87	85	96	94

The fully automated syntheses comprised of the preparation of [^{11}C]CH_3I, reaction with the respective precursor, semi-preparative purification as well as formulation to physiological conditions was set up for compounds **3a**, **3b**, **3c**, **3i**, **3j** and **3k**. Although the small-scale reaction showed complete conversion at room temperature in DMSO, for the fully-automated synthesis the reaction temperature was increased to 80 °C, because unreacted [^{11}C]CH_3I was observed during semi-preparative HPLC of the crude reaction mixture at 20 °C for all compounds. Precursor **2k** features two potential nucleophilic sites that could react with [^{11}C]CH_3I (see Supporting Information).

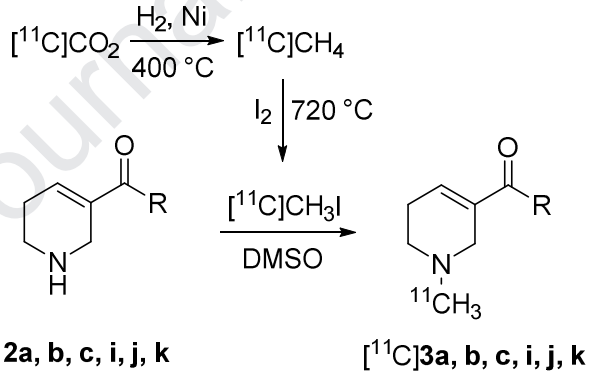

Figure 7: Reaction scheme of the radiochemical labeling.

In total 32 large-scale batches of carbon-11 compounds were produced (Table 5). Due to different semi-preparative HPLC runtimes the overall synthesis time from end of bombardment varies slightly among the products and ranges between 40-45 min, which is approximately two half-lives of carbon-11 ($t_{1/2}$ = 20 min). Precursors (**2**) were employed in a roughly 100-fold excess compared to [^{11}C]CH_3I. The radiochemical purity as determined by HPLC exceeded 96 % in all batches and pH and osmolality were determined to be in the physiological range. All radiolabeled compounds showed high purity

and physico-chemical parameters as determined in the quality control were in accordance with the guidelines of the European Pharmacopoeia for radiopharmaceutical preparations.[37]

Table 5: Production parameters of carbon-11-labeled compounds. Yield is related to the estimated starting activity of $[^{11}C]CO_2$.

	[^{11}C]**3a**	[^{11}C]**3b**	[^{11}C]**3c**	[^{11}C]**3i**	[^{11}C]**3j**	[^{11}C]**3k**
n	3	5	19	2	1	2
yield (GBq)	5.9±1.0	5.3±1.6	3.8±1.3	2.7±2.0	7.2	4.3±1.0
RCY (%)	18.7±2.7	17.4±6.8	12.9±3.8	8.6±4.8	21.1	13.2±2.4
A_m at EOS (GBq/µmol)	58±17	93±80	122±115	30±6	43	132±36

We showed that **3a**-**c** and **3i**-**k** can be carbon-11 labelled straightforwardly in high yields, independent of the carbonyl substituent (R). The high yields of the radiosynthesis of all tested compounds enable a potential application for at least two patients per synthesis.

Physico-chemical parameters and pharmacological behavior of radiolabeled compounds

Human liver microsome metabolism was studied with compounds [^{11}C]**3b**, [^{11}C]**3c** and [^{11}C]**3i**. For all of them the main radiometabolite was identified as [^{11}C]arecaidine and the rate of its formation was found out to be heavily dependent on the structure of the parent compound (Figure 8). [^{11}C]**3i** was almost unaffected by human liver microsomes, whereas 30 % [^{11}C]**3b** and 53 % [^{11}C]**3c** were unmetabolized after 1 h. Furthermore, a second radiometabolite with a retention time between arecaidine and the parent compound was observed for all three compounds (Supporting Information, Table S2, Figure S8). This metabolite never represented more than 10 % of the total activity and was identified as arecaidine ethyl ester ($C_9H_{15}NO_2$), based on HPLC-HRMS measurements (Supporting Information) of nonradioactive incubations of **3b** with human liver microsomes. Formation of the ethyl ester can be explained by the presence of EtOH in the tracer formulation. *In*

vivo experiments are expected to be unaffected by [^{11}C]arecaidine ethyl ester formation, rationalized by the concomitant stronger dilution of EtOH. Considering the expected low transport of [^{11}C]arecaidine across the blood brain barrier[38] and the low affinity to all mAChRs, we are confident that ester cleavage in the liver will not interfere with neuroimaging but can potentially affect applications in the peripheral nervous system.

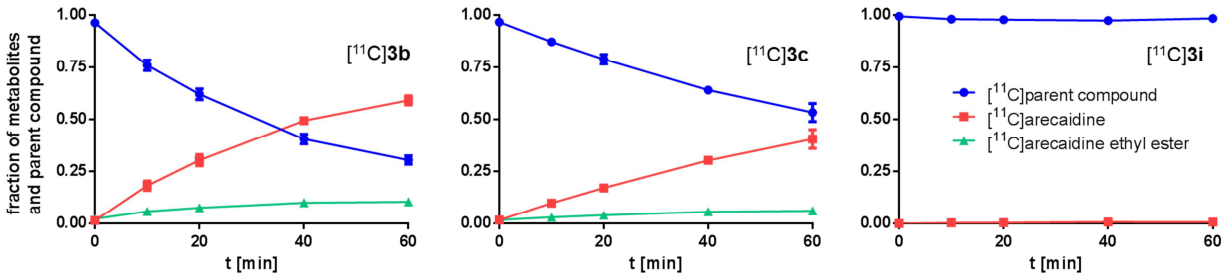

*Figure 8: Metabolic stability of compounds [^{11}C]**3b**, [^{11}C]**3c** and [^{11}C]**3i** against human liver microsomes. Error bars represent standard deviation of n=3 ([^{11}C]**3b** and [^{11}C]**3c**) or n=2 ([^{11}C]**3i**) incubations of individual batches.*

Serum protein binding of [^{11}C]**3b**, [^{11}C]**3c** and [^{11}C]**3i** was studied by ultrafiltration, demonstrating 5.8±1.0 %, 9.0±1.2 % and 18.2±0.4 % (n≥3, ±sd) free fraction, respectively. The measured serum protein binding is comparable to established brain tracers[39], substantiating the possible utilization of [^{11}C]**3b**, [^{11}C]**3c** and [^{11}C]**3i** for *in vivo* imaging. Plasma stability of [^{11}C]**3c** was 94±2% after 60 min (n=3).

To reduce tracer metabolism, we exchanged the ester for an amide bond (**3i**), which resulted in drastic improvement of metabolic stability. However, the mAChR affinity of **3i** is much lower compared to its bioisostere **3b**. To sum it up, [^{11}C]**3b** and [^{11}C]**3c** represent the most promising substances of this series regarding mAChR PET tracer development. Comparing these two, [^{11}C]**3c** stands out, because of its higher *in vitro* metabolic stability and M1 subtype selectivity.

Interactions of [^{11}C]3c with CHO-M1 cells

The kinetics of the interaction of [^{11}C]**3c** with living CHO-M1 cells was studied using LigandTracer. On the first view promising binding curves, reaching equilibrium in 8 to 15 min, were obtained. However,

the observed binding did not reach saturation at a concentration 100-fold above K_i but showed a rather linear equilibrium signal increase with concentration (maximum concentration of 10× K_i shown in Figure S9A for the sake of readability). Furthermore, CHO-M1 cells preblocked with 10 µM scopolamine showed essentially the same binding kinetics as unblocked CHO-M1 cells Figure S9A). Additionally, the binding curvature appeared independent on [^{11}C]**3c** concentration (Figure S9B). Considering these observations, we concluded that the binding observed in the LigandTracer experiments cannot exclusively be explained by the interaction of **3c** with mAChR M1.

To study this further, we performed a direct radioligand binding assay using [^{11}C]**3c** and investigated the binding behavior of blocked CHO-M1 cells versus unblocked CHO-M1 cells at three different concentrations in six-well plates (Figure 9). At a radioligand concentration of 0.3 nM blocking with 10 µM scopolamine and 10 µM pirenzepine significantly reduced the binding of [^{11}C]**3c** to CHO-M1 cells. However, CHO cells lacking the M1 receptor (blank) show an overall lower radioligand binding compared to the blocked CHO-M1 cells. Hence, the observed [^{11}C]**3c** binding is not fully blockable with the used concentrations and reference ligands. With increasing concentrations of **3c** blocking with scopolamine and pirenzepine becomes less effective, leading to no significant difference in radioligand binding between unblocked and blocked CHO-M1 cells at 3 nM and 30 nM of **3c**.

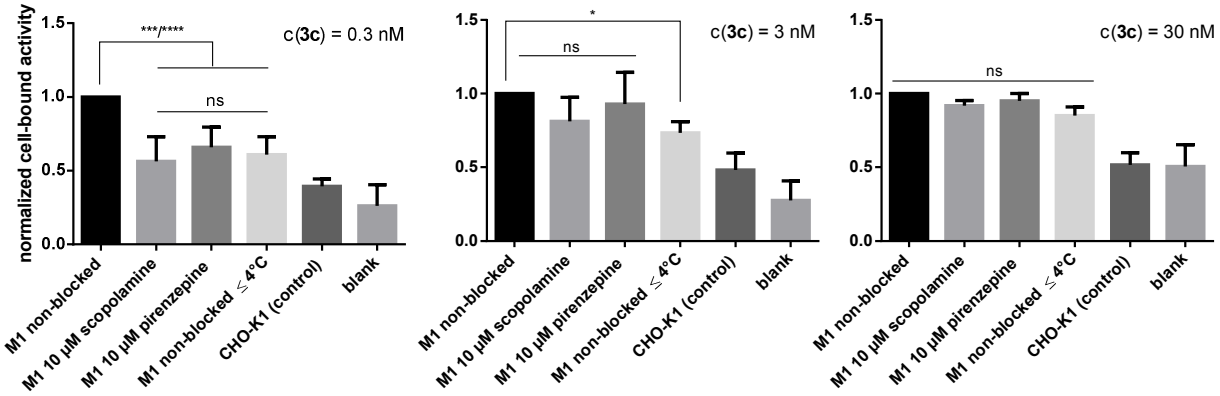

*Figure 9:[^{11}C]**3c** binding to CHO cells. Data are displayed normalized to the binding on the non-blocked CHO-M1 cells. Groups were compared using an ordinary one-way ANOVA and Tukey's multiple comparisons test, with a single pooled variance (*:*

*P ≤ 0.05, ***: P ≤ 0.001, ****: P ≤ 0.0001, ns: not significant, n ≥ 3). At all tested [^{11}C]**3c** concentrations the normalized cell-bound activity of the CHO-K1 control cells was not significantly different from the blank.*

As control, the similar assay was performed at ≤ 4 °C to investigate the ligand binding without active process contributions (Figure 9).[40] At CHO-M1 cells ≤ 4 °C [^{11}C]**3c** binding is reduced to the same extent as in blocked CHO-M1 cells, indicating that active cellular processes are involved in the binding of [^{11}C]**3c** to living cells.

The extent of specific binding is limited to the amount of expressed target, whereas nonspecific binding increases linearly with the radioligand concentration and is not saturable. Thus, the specific binding was only visible at a low radioligand concentration (0.3 nM), while at higher concentrations (3 nM, 30 nM) mostly nonspecific binding was detected.

***In vitro* autoradiography**

Total binding of [^{11}C]pirenzepine (15 nM) was reduced to background signal in the presence of 10 µM scopolamine or atropine confirming that the brain sections and the used procedure allows the visualization of specific binding to mAChRs. However, neither of the blocking agents significantly reduced the radioactive signal derived from total [^{11}C]**3c** (30 nM) binding in a total of 30 brain sections derived from different brain regions of two different subjects, demonstrating only nonspecific binding (Figure 10).

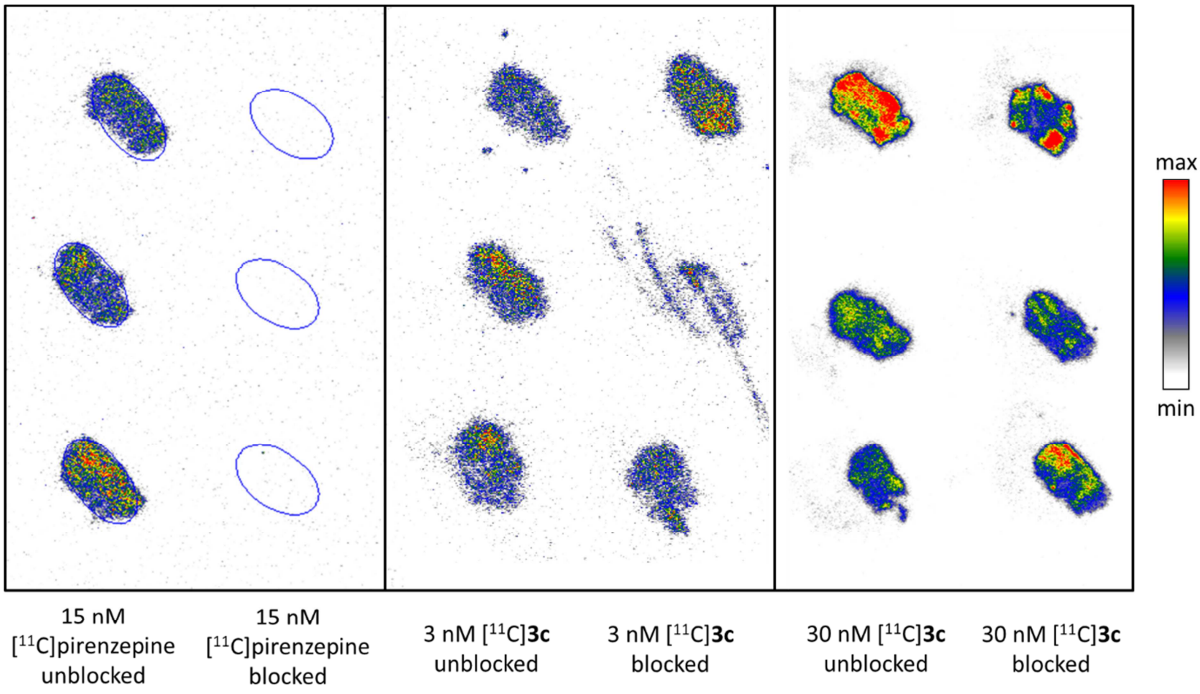

Figure 10: Autoradiography of mice brain sections. Blocking was performed by co-incubation with 10 µM scopolamine. The signal at 15 nM [^{11}C]pirenzepine blocked is below limit of detection and the position of the invisible sections is therefore marked with a blue ellipse. Radioactivity is displayed as a linear color gradient. Sections separated in boxes are derived from different experiments, allowing only semi-quantitative analysis.

Also at a concentration close to the K_D [^{11}C]**3c** (3 nM) did not show a difference between baseline and blocking, whereas [^{11}C]pirenzepine at a concentration close to the K_D (15 nM) clearly showed specific binding.

Conclusion

Despite the pivotal role of mAChRs in human physiology and disease, non-invasive external imaging thereof has not yet found its way into clinical routine. Constrained imaging properties of the currently available mAChR PET tracers demand improvement in order to correspond to the clinical needs. In search of an improved PET tracer for mAChRs fifteen novel arecoline-derived compounds were synthesized, characterized and tested for their affinity toward mAChRs and EeAChE. Conjugation of arecaidine to diphenylmethyl-containing structures afforded K_i values in the low nanomolar range, which is suitable for the application as mAChR PET probe. Besides, the difference in affinity of (+)-**3e** and (-)-**3e** underline the applicability of stereochemistry to impact mAChR M1

ligand development. Moreover, all tested compounds were shown to neither act as orthosteric ligand nor substrate for the off-target AChE. Fully-automated carbon-11-labeling procedures for [^{11}C]**3a**-**c** and [^{11}C]**3i**-**k** were developed and the most promising candidates underwent further studies to assess their metabolic stability and serum protein binding, where [^{11}C]**3b** and [^{11}C]**3c** showed suitable properties for future tracer development. Real-time and endpoint radioligand binding studies using [^{11}C]**3c** on living cells as well as *in vitro* autoradiography on mouse brain sections revealed pronounced nonspecific binding, which motivates us to reduce the lipophilicity for future tracer candidates of similar structure prior to *in vivo* studies. Although the observed nonspecific binding of [^{11}C]**3c** restrains this compound from acting as imaging agent, it can still be considered as mAChR M1 ligand for purposes where nonspecific binding is less of a problem, *e.g.* therapeutics.[41]

Experimental Section

Materials

Diphenylmethyl trichloroacetimidate[42], furan-2-yl(phenyl)methanol[43], arecaidine[44] and *N*-Boc-guvacine[44] were synthesized as published previously. *N*-Fmoc-guvacine (≥ 98 %, Santa Cruz Biotechnology), arecoline hydrobromide (XA BC-Biotech), scopolamine hydrobromide (Sigma-Aldrich), pirenzepine dihydrochloride (≥ 98 %, Sigma-Aldrich), diethylamine (DEA, > 99 %, Fisher Scientific), thionylchloride (≥ 99 %, Sigma-Aldrich), triethylene glycol monomethyl ether (95 %, Aldrich), diphenylmethanol (99 %, Aldrich), 4,4'-dimethoxybenzhydrol (98+%, Alfa Aesar), 4,4'-difluorobenzhydrol (98+%, Alfa Aesar), (4-bromophenyl)(4-fluorophenyl)methanol (fluorochem), benzhydrylamine (97 %, Alfa Aesar), *N*,*N*'-dicyclohexycarbodiimide (DCC, 99 %, Alfa Aesar), 1,1'-carbonyldiimidazole (CDI, reagent grade, Sigma Aldrich), iodomethane (CH_3I, ≥ 99 %, Sigma-Aldrich), trichloroacetonitrile (98 %, Alfa Aesar), 1,8-diazabicyclo[5,4,0]undec-7-en (> 97 %, Merck-Schuchardt), 11-(chloroacetyl)-5,11-dihydro-6H-pyrido[2,3-b][1,4]benzodiazepine-6-one (abcr), trifluoroacetic acid (99 %, Alfa Aesar), aq. HBr (48 %, Sigma Aldrich), formic acid (≥ 95 %, Merck), 2-chloroacrylonitrile (98 %, Sigma Aldrich), 2-(methylamino)ethanol (99 %, Alfa Aesar), KO^{t}Bu (≥ 98 %,

Sigma Aldrich), 5,5'-dithiobis-(2-nitrobenzoic acid) (DTNB, ≥98 %, Carl Roth), acetylthiocholine iodide (ATI, ≥ 98 %, Sigma Aldrich), tacrine hydrochloride (≥98 %, Santa Cruz Biotechnology), acetylcholinesterase from *Electrophorus electricus* (1323 units/mg, Sigma Aldrich), sodium hydride (NaH, 60 % dispersion in mineral oil, Aldrich), Mg turnings (≥ 99 %, Sigma Aldrich), benzyl chloride (> 99 %, Merck), 5-bromo-2-fluoropyridine (> 98 %, TCI), ethyl formate (97 %, Sigma Aldrich), dibromoethane (> 98 %, Merck), sodium carbonate (Na_2CO_3, anhydrous for analysis, Merck), sodium bicarbonate ($NaHCO_3$, ≥ 98 %, Fluka), sodium iodide (NaI, 99.5 %, Merck), poly(ethyleneimine) (PEI, 50 % in H_2O, Fluka), *N*,*N*-dimethylformamide (DMF, 99.8 % extradry over molecular sieve, Acros), acetonitrile (ACN, Sigma Aldrich), dichloromethane (DCM, EMPROVE® ESSENTIAL, Merck), *n*-hexane (PE, Hi-PerSolv CHROMANORM, VWR), ethyl acetate (EE, 99.9 %, VWR), diethyl ether (Et_2O, 100 %, VWR), ethanol (EMROVE® exp, Merck), dimethylsulfoxide (DMSO, ≥ 99.9 %, Sigma Aldrich) and C18 Sep-Pak (WAT020515, Waters) cartridges were purchased and used as received. Solvents indicated as "dry" were stored over molecular sieves for a minimum of 2 days. Reaction progress was monitored by pre-coated TLC sheets ALUGRAM® Xtra SIL G/UV254 (0.20 mm silica gel 60 with fluorescent indicator). Silica gel on TLC plates (0.25 mm, 20x20 cm, 99571 Sigma Aldrich) was used for preparative separation unless stated otherwise. In indicated cases aluminiumoxide 60 F_{254} neutral (Merck) was used for preparative TLC. [*N*-methyl-^{3}H]scopolamine methyl chloride (2.964 TBq/µmol, 37 MBq, in 1 mL ethanol) was purchased from PerkinElmer.

Instrumentation

NMR samples were measured in chloroform-d ($CDCl_3$, ≥ 99.8 %, stabilized with silver foil, Sigma Aldrich) at 25 °C. The center of the (residual) solvent signal was used as an internal standard which was related to TMS with δ 7.26 ppm (^{1}H in $CDCl_3$) and δ 77.0 ppm (^{13}C in $CDCl_3$). ^{19}F NMR spectra were referenced *via* Ξ ratio and gsHMBC spectra of ^{15}N were referenced against neat, external CH_3NO_2. Unless stated otherwise full and unambiguous assignment of NMR signals was achieved by

combination of standard NMR techniques, such as COSY, NOESY, APT, HSQC and HMBC experiments. NMR spectra of intermediates were recorded with a Bruker Avance III 200 spectrometer (200 MHz for ^{1}H). NMR spectra of final compounds were recorded with a Bruker Avance III 400 spectrometer (400 MHz for ^{1}H, 100 MHz for ^{13}C, 40 MHz for ^{15}N and 376 MHz for ^{19}F) or a Bruker Avance III 600 spectrometer (600 MHz for ^{1}H, 150 MHz for ^{13}C and 565 MHz for ^{19}F). Mass spectra were obtained on a Bruker maXis 4G instrument (ESI-TOF, HRMS). All newly synthesized or tested compounds (**1a**-**8**) passed a pan assay interference compounds filter.[45] An Agilent 1260 Infinity HPLC System with a flow of 1 mL/min and XBridge Shield RP18 2.5 µm, 50 x 3.0 mm column was used for determination of the radiochemical yield in the small scale reactions, quality control of the radiotracers as well as for the assessment of the tracer stability in formulation (further parameters shown in Table 6). LogP measurements were performed and interpreted as published recently[31] on an Agilent HPLC system consisting of an autosampler (series 1100), pump (series 1200), diode array detector (series 1100) and a radiodetector (Ramona, Elysia-Raytest) using an apHERA (5 µm, 10 x 6 mm) stationary phase. All tested compounds (**3a**-**m**, **6**-**8**) were shown to have a purity exceeding 95 % as analyzed by the logP HPLC method without addition of toluene and triphenylene. The same HPLC System was used for the analysis of human liver microsomes metabolites with an XSelect^{TM} (HSS T3, 3.5 µm, 100 x 4.6 mm) stationary phase, a flow of 1 mL/min and a gradient program (0.0-3.0 min: 95 % pH 9.3, 5 % ACN; 5.0-14.0 min: X % pH 9.3, 100-X % ACN; 15.0-16.0 min: 95 % pH 9.3, 5 % ACN; with X being 50, 45 and 63 for compounds **3b**, **3c** and **3i**, respectively). For the analysis of EeAChE metabolism a similar gradient was used: 0.0-3.0 min: 98 % pH 9.3, 2 % ACN; 5.0-14.0 min: 40 % pH 9.3, 60 % ACN; 15.0-16.0 min: 98 % pH 9.3, 2 % ACN. The used eluent buffer is a 25 mM $NH_4H_2PO_4$ solution set to pH 9.3 with NaOH. The LOQ given in Table 6 was estimated based on the standard deviation of the response and the slope.[46]

*Table 6: Separation conditions for analytical HPLC as part of radiotracer quality control and for the concentration determination of the **3e** enantiomers.*

Compound	Eluent	$k_{prec.}$	$k_{prod.}$	LOQ [µg/mL]

3a	20% ACN, 80% pH 9.3	1.20	2.67	0.88
3b	60% ACN, 40% pH 9.3	2.00	3.53	1.05
3c	60% ACN, 40% pH 9.3	1.93	3.73	1.07
3e	75% ACN, 25% pH 9.3	-	2.35	1.20
3i	40% ACN, 60% pH 9.3	2.53	4.60	1.83
3j	20% ACN, 80% pH 9.3	1.80	3.67	1.99
3k	50% ACN, 50% pH 9.3	1.53	2.67	0.76

CHO-K1 cells stably transfected with human muscarinic receptors M1-M5 were obtained from Missouri University of Science and Technology cDNA Resource Center (Cell Catalog#: CEM1000000, CEM2000000, CEM3000000, CEM4000000, CEM5000000) and cultivated in Ham's F12 Nutrient Mixture (Gibco, Life Technologies Limited) containing 10 % FBS (Gibco, Life Technologies Limited), 250 µg/mL Geneticin® (G418, Thermo Fisher) at 37 °C and 5 % CO_2 in a cell incubator. Gibco™ Trypsin-EDTA (0.05%) was used for passaging cells. Untransfected CHO-K1 cells were obtained from ATCC and cultivated like described above but in media free of Geneticin®. Protease Inhibitor Cocktail powder (P2714-1BTL, Sigma-Aldrich) was dissolved in 10 mL water and used as such. The protein concentration of membrane suspensions was determined with Pierce™ BCA Protein Assay Kit (Thermo Scientific) on a BioTek Synergy HTX multi-mode reader. A M-36 tygon tubed Cell Harvester (Brandel®) and Whatman™ GF/B filters were used for the filtration of radioligand binding assays. Filter disks were counted with 2 mL Ultima Gold™ (high flashpoint LSC cocktail, PerkinElmer) using a 300 SL Automatic TDCR liquid Scintillation Counter (HIDEX) in CPM mode. LigandTracer grey and yellow (ridgeview instruments ab, Sweden) with LigandTracer Control V2.0.1 and TraceDrawer V1.8.1 were used for measuring real-time kinetic on living cells.

A GE PETtrace 860 cyclotron (General Electric Medical System, Sweden) was used for the production of $[^{11}C]CO_2$ by a $^{14}N(p, \alpha)^{11}C$ reaction in gas target filled with N_2 + 1% O_2 (Topline, Messer) at a beam current of 65 µA. Transformation to $[^{11}C]CH_3I$, radiolabeling of the precursor and tracer purification

were carried out in a TRACERlab™ FX C Pro synthesizer using the built in semi-preparative HPLC system featuring a Linear Instruments Model 200 UV/Vis detector and a LaPrep HPLC pump (VWR).[47]

Table 7: Separation conditions for semi-preparative HPLC during radiosynthesis.

Compound	Column	Eluent	Flow [mL/min]	$k_{prec.}$	$k_{prod.}$
3a	Supelcosil™ LC-ABZb, 5 µm, 250 × 10 mm	15% ACN, 85% pH 9.3	5.0	3.25	4.88
3j		20% ACN, 80% pH 9.3	5.0	1.70	2.37
3b	Supelcosil™ LC-ABZb, 5 µm, 250 × 10 mm	50% ACN, 50% pH 9.3	5.0	2.63	4.60
3c		50% ACN, 50% pH 9.3	7.5	3.12	4.60
3i	Nucleodur PolarTec, 5 µm, 250 x 10 mm	45% ACN, 55% pH 9.3	5.0	2.60	3.92
3k	ProntoSIL 120 C18 ace-EPS, 5 µm, 250 x 10 mm	60% ACN, 40% pH 6.8	5.0	1.75	3.33

Metabolic stability was studied with Corning® Gentest™ HLM, ~20-Donor Pool, Mixed Gender microsomes and Corning® Gentest™ NADPH Regenerating System, Solution A and B. Pooled Human Serum (Innovative Research, Inc.), Centrifree®, Ultracel®PL Regenerated Cellulose Centrifugal filters (Merck Millipore), Microcon®-10 Ultracel®PL-10 Regenerated Cellulose 10,000 NMWL Centrifugal Filters and a 2480 Wizard^2 Automatic Gamma Counter (Perkin Elmer) were used for determination of serum protein binding.

Synthesis

1-(9*H*-fluoren-9-yl)methyl 3-methyl 1,2,5,6-tetrahydropyridine-1,3-dicarboxylate (*N*-Fmoc-guvacoline) (1a). *N*-Fmoc-guvacine (50.0 mg, 0.143 mmol) and Na_2CO_3 (18.2 mg, 0.172 mmol) were

suspended in dry DMF (5 mL) for 30 min at 20 °C. CH_3I (100 µL, 1.61 mmol) was added dropwise and the reaction mixture was stirred o/n. The reaction mixture was poured on H_2O (60 mL) and extracted with Et_2O (3x 30 mL). The combined organic layers were washed with H_2O (2x 15 mL), dried with Na_2SO_4, filtered and evaporated to give **1a** (49.8 mg, 96 %) as a highly viscous oil.

^{1}H-NMR (200MHz, $CDCl_3$) δ 7.77 (d, *J*=7.3Hz, 2H), 7.59 (d, *J*=7.3Hz, 2H), 7.40 (t, *J*=7.3Hz, 2H), 7.31 (t, *J*=7.3Hz, 2H), 7.08 (s, 1H), 4.46 (d, *J*=6.8Hz, 2H), 4.27 (t, *J*=6.8Hz, 1H), 4.22-4.17 (m, 2H), 3.79 (s, 3H), 3.52 (brs, 2H), 2.29 (brs, 2H).

methyl 1,2,5,6-tetrahydropyridine-3-carboxylate (guvacoline) (2a). 1a (49.8 mg, 0.137 mmol) was dissolved in ACN (3 mL), diethylamine (300 µL, 2.91 mmol) was added and the reaction mixture was stirred for 2.5 h at 20 °C. The reaction mixture was evaporated to about 1 mL and the product was isolated by preparative TLC (PE:EE = 1:6 + 1% DEA; R_f = 0.13-0.33) and appeared as yellowish oil (17.9 mg, 93 %).

^{1}H-NMR (400MHz, $CDCl_3$) δ 7.04 (m, 1H, H-4), 3.73 (s, 3H, O-CH_3), 3.55 (m, 2H), 2.93 (t, *J*=5.7Hz, 2H, H-6), 2.28-2.21 (m, 2H, H-5).* ^{13}C-NMR (100MHz, $CDCl_3$) δ 166.5 (C=O), 138.3 (C-4), 130.3 (C-3), 51.5 (O-CH_3), 44.1 (C-2), 41.9 (C-6), 26.2 (C-5). HRMS (ESI) calcd for $C_7H_{12}NO_2$ (M + H^+) 142.0863, found 142.0876. *The guvacoline ^{1}H NH signal could not be found.

3-benzhydryl 1-(9*H*-fluoren-9-yl)methyl 1,2,5,6-tetrahydropyridine-1,3-dicarboxylate (1b). *N*-Fmoc-guvacine (50.0 mg, 0.143 mmol) and diphenylmethyl trichloroacetimidate (61.1 mg, 0.186 mmol) were dissolved in dry DCM (2 mL) and stirred at 20 °C under argon for 16 h. The product was isolated *via* preparative TLC (PE:EE = 3:1; R_f = 0.25-0.56) and formed white crystals (64.3 mg, 87 %).

^{1}H-NMR (200MHz, $CDCl_3$) δ 7.74 (brs, 2H), 7.58 (brs, 2H), 7.46-7.20 (m, 14H), 6.99 (brs, 1H), 4.52-4.05 (m, 5H), 3.54 (brs, 2H), 2.32 (brs, 2H), 2.06 (s, 1H).

benzhydryl 1,2,5,6-tetrahydropyridine-3-carboxylate (2b). 1b (64.3 mg, 0.125 mmol) was dissolved in ACN (3 mL), diethylamine (300 µL, 2.91 mmol) was added and the reaction mixture was stirred for 2 h at 20 °C. The reaction mixture was evaporated to about 1 mL and the product was isolated by preparative TLC (PE:EE = 1:1 + 1% DEA; R_f = 0.12-0.28) and appeared as yellowish wax (32.5 mg, 89 %).

^{1}H-NMR (400MHz, $CDCl_3$) δ 7.34 (m, 8H, Ph H-2,3,5,6), 7.28 (m, 2H, Ph H-4), 7.20 (m, 1H, H-4), 6.94 (s, 1H, $CHPh_2$), 3.65 (m, 2H, H-2), 2.96 (t, *J*=5.7Hz, 2H, H-6), 2.30 (m, 2H, H-5).* ^{13}C-NMR (100MHz, $CDCl_3$) δ 164.7 (C=O), 140.3 (Ph C-1), 138.9 (C-4), 130.0 (C-3), 128.5 (Ph C-3,5), 127.9 (Ph C-4), 127.0 (Ph C-2,6), 76.7 ($CHPh_2$), 43.8 (C-2), 41.7 (C-6), 26.0 (C-5). HRMS (ESI) calcd for $C_{19}H_{20}NO_2$ (M + H^+) 294.1489, found 294.1487. *The guvacoline ^{1}H NH signal could not be found.

bis(4-fluorophenyl)methyl 2,2,2-trichloroacetimidate. Bis(4-fluorophenyl)methanol (220 mg, 1.00 mmol), trichloroacetonitrile (10.0 mL, 10.0 mmol) and 1,8-diazabicyclo(5.4.0)undec-7-ene (0.10 mmol, 15 µL) were stirred in dry DCM at 20 °C under argon for 1.5 h. Volatiles were evaporated and the residue was purified by silica column chromatography (PE:EE = 80:1 + 3 % TEA). The product appeared as white crystals (358 mg, 98 %).

^{1}H-NMR (200MHz, $CDCl_3$) δ 8.45 (brs, 1H), 7.45-7.32 (m, 4H), 7.13-6.98 (m, 4H), 6.92 (s, 1H).

bis(4-fluorophenyl)methyl 1-(2-(9*H*-fluoren-9-yl)acetyl)-1,2,5,6-tetrahydropyridine-3-carboxylate (1c). *N*-Fmoc-guvacine (40.0 mg, 0.115 mmol) and bis(4-fluorophenyl)methyl 2,2,2-trichloroacetimidate. (54.2 mg, 0.149 mmol) were dissolved in dry DCM (3 mL) and stirred at 20 °C under argon for 16 h. The product was isolated *via* preparative TLC (PE:EE = 7:2; R_f = 0.26-0.51) and formed white crystals (57 mg, 93 %).

^{1}H-NMR (200MHz, $CDCl_3$) δ 7.74 (brs, 2H), 7.57 (d, *J*=7.4Hz, 2H), 7.44-7.18 (m, 9H), 7.10-6.98(m, 4H), 6.94 (s, 1H), 4.50-4.38 (m, 2H), 4.32-4.21 (m, 3H), 3.53 (brs, 2H), 2.33 (brs, 2H).

bis(4-fluorophenyl)methyl 1,2,5,6-tetrahydropyridine-3-carboxylate (2c). 1c (57.1 mg, 0.107 mmol) was dissolved in ACN (3 mL), diethylamine (300 µL, 2.91 mmol) was added and the reaction mixture was stirred for 2 h at 20 °C. The reaction mixture was evaporated to about 1 mL and the product was isolated by preparative TLC (PE:EE = 1:1 + 1% DEA; R_f = 0.08-0.25) and appeared as yellowish oil (23.7 mg, 63 %).

^{1}H-NMR (400MHz, $CDCl_3$) δ 7.29 (m, 4H, Ph H-2,6), 7.18 (m, 1H, H-4), 7.03 (m, 4H, H-3,5), 6.89 (s, 1H, $CHPh_2$), 3.64 (m, 2H, H-2), 2.97 (t, *J*=5.8Hz, 2H, H-6), 2.33 (m, 2H, H-5).* ^{13}C-NMR (100MHz, $CDCl_3$) δ 164.5 (C=O), 162.4 (d, *J*=247.1Hz, Ph C-4), 139.2 (C-4), 135.9 (d, *J*=3.2Hz, Ph C-1), 129.6 (C-3), 128.8 (d, *J*=8.2Hz, Ph C-2,6), 115.5 (d, *J*=21.7Hz, Ph C-3,5), 75.5 ($CHPh_2$), 43.7 (C-2), 41.6 (C-6), 25.9 (C-5). ^{19}F-NMR (377MHz, $CDCl_3$) δ -113.9 (m, Ph-F). HRMS (ESI) calcd for $C_{19}H_{18}F_2NO_2$ ($M + H^+$) 330.1300, found 330.1302. *The guvacoline ^{1}H NH signal could not be found.

***tert*-butyl 5-(benzhydrylcarbamoyl)-1,2,3,6-tetrahydropyridine-1-carboxylate (1i).** *N*-Boc-guvacine (40.0 mg, 0.176 mmol) and CDI (28.5 mg, 0.176 mmol) were stirred in dry THF (3 mL) at 20 °C under argon for 30 min. Benzhydrylamine (45 µL, 0.264 mmol) was added and the reaction was stirred for 72 h. The reaction mixture was evaporated to 0.5 mL, the formed precipitate was removed by filtration and the filtrate purified *via* preparative TLC (PE:EE = 5:2; R_f = 0.32-0.49). The product appeared as colorless oil (8.0 mg, 12 %).

^{1}H-NMR (200MHz, $CDCl_3$) δ 7.40-7.16 (m, 10H), 6.64 (brs, 1H), 6.34-6.14 (m, 2H), 4.22-4.12 (m, 2H), 3.49 (t, *J*=5.6Hz, 2H), 2.34-2.20 (m, 2H), 1.46 (s, 9H).

***N*-(diphenylmethyl)-1,2,5,6-tetrahydropyridine-3-carboxamide (2i). 1i** (8.0 mg, 0.020 mmol) was stirred in DCM (2 mL) containing TFA for 1.5 h at 20 °C. The volatiles were removed by evaporation, the solid residue was taken up in saturated Na_2CO_3 solution and extracted with DCM (3x 2 mL). The extract was dried with Na_2SO_4, filtered and evaporated to yield a colorless oil (4.7 mg, 79 %).

^{1}H-NMR (400MHz, $CDCl_3$) δ 7.33 (m, 4H, Ph H-3,5), 7.27 (m, 2H, Ph H-4), 7.23 (m, 4H, Ph H-2,6), 6.62 (m, 1H, H-4), 6.29 (d, *J*=7.8Hz, 1H, $CHPh_2$), 6.21 (brd, *J*=7.8Hz, 1H, CONH), 3.61 (m, 2H, H-2), 2.93 (t, *J*=5.7Hz, 2H, H-6), 2.21 (m, 2H, H-5).* ^{13}C-NMR (100MHz, $CDCl_3$) δ 166.2 (C=O), 141.5 (Ph C-1), 134.2 (C-3), 131.1 (C-4), 128.7 (Ph C-3,5), 127.5 (Ph C-4), 127.4 (Ph C-2,6), 56.8 ($CHPh_2$), 44.3 (C-2), 42.1 (C-6), 25.7 (C-5). ^{15}N-NMR (41MHz, $CDCl_3$) δ -260.2 (CONH).** HRMS (ESI) calcd for $C_{19}H_{21}N_2O$ ($M + H^+$) 293.1648, found 293.1649. *The guvacoline ^{1}H NH signal could not be found. ** The guvacoline ^{15}N signal could not be found.

1-(9*H*-fluoren-9-yl)methyl 3-{2-[2-(2-methoxyethoxy)ethoxy]ethyl} 1,2,5,6-tetrahydropyridine-1,3-dicarboxylate (1j). *N*-Fmoc-guvacine (50.0 mg, 0.143 mmol) was suspended in dry DCM (2 mL) and $SOCl_2$ (250 µL, 3.45 mmol) was added by syringe. The mixture was sonicated for 40 min at 20 °C. Evaporation of the volatiles yielded the acyl chloride, which was heated to 50 °C with triethylene glycol monomethyl ether (1 mL, 6.25 mmol) for 1 h. The reaction mixture was poured on H_2O (30 mL) and extracted with Et_2O (5x 15 mL). The combined organic layers were washed with H_2O (2x 10 mL), dried with Na_2SO_4, filtered and evaporated to give **1j** (66.0 mg, 93 %) as a viscous, slightly yellow oil.

^{1}H-NMR (200MHz, $CDCl_3$) δ 7.76 (d, *J*=7.2Hz, 2H), 7.58 (d, *J*=7.2Hz, 2H), 7.40 (t, *J*=7.2Hz, 2H), 7.31 (t, *J*=7.2Hz, 2H), 7.10 (s, 1H), 4.45 (d, *J*=6.3Hz, 2H), 4.38-4.18 (m, 5H), 3.80-3.47 (m, 12H), 3.37 (s, 3H), 2.29 (brs, 2H).

2-[2-(2-methoxyethoxy)ethoxy]ethyl 1,2,5,6-tetrahydropyridine-3-carboxylate (2j). 1j (66.0 mg, 0.133 mmol) was dissolved in ACN (3 mL), diethylamine (300 µL, 2.91 mmol) was added and the

reaction mixture was stirred for 2 h at 20 °C. The reaction mixture was evaporated to about 1 mL and the product was isolated by preparative TLC (EE + 1% DEA; R_f = 0.14-0.48) and appeared as yellowish oil (31.8 mg, 87 %).

^{1}H-NMR (400MHz, $CDCl_3$) δ 7.07 (m, 1H, H-4), 4.29 (m, 2H, TEG H-1), 3.73 (m, 2H, TEG H-2), 3.68-3.63 (m, 6H, TEG H-3,4,5), 3.55 (m, 2H, H-2), 3.54 (m, 2H, TEG H-6), 3.38 (s, 3H, OCH_3), 2.92 (t, *J*=5.7Hz, 2H, H-6), 2.27-2.20 (m, 2H, H-5).* ^{13}C-NMR (100MHz, $CDCl_3$) δ 165.9 (C=O), 138.6 (C-4), 130.3 (C-3), 71.9 (TEG C-6), 70.62 (TEG C-3)**, 70.61 (TEG C-4)**, 70.57 (TEG C-5), 62.9 (TEG C-2), 59.0 (OCH_3), 44.0 (C-2), 41.9 (C-6), 26.2 (C-5). HRMS (ESI) calcd for $C_{13}H_{24}NO_5$ ($M + H^+$) 274.1649, found 274.1647. *The guvacoline ^{1}H NH signal could not be found. **indistinguishable

(9*H*-fluoren-9-yl)methyl 5-{[3-cyclohexyl(cyclohexylcarbamoyl)amino]carbonyl}-1,2,3,6-tetrahydropyridine-1-carboxylate (1k). *N*,*N*'-Dicyclohexylcarbodiimide (20.7 mg, 0.100 mmol) was added to a stirred solution of *N*-Fmoc-guvacine (31.9 mg, 0.0913 mmol) in 1 mL dry DMF at 20 °C. After 1.5 h more *N*,*N*'-Dicyclohexylcarbodiimide (10.0 mg, 0.0483 mmol) was added. After 20 h the reaction mixture was poured on water (10 mL) and extracted with Et_2O (3x 10 mL). The combined organic layers were dried with Na_2SO_4, filtered, evaporated and purified *via* preparative TLC (PE:EE = 2:1; R_f = 0.44-0.66). The product was obtained as white, crystalline solid (24.4 mg, 48 %).

^{1}H-NMR (200MHz, $CDCl_3$) δ 7.77 (d, *J*=7.2Hz, 2H), 7.58 (d, *J*=7.2Hz, 2H), 7.40 (t, *J*=7.2Hz, 2H), 7.31 (t, *J*=7.2Hz, 2H), 6.25 (brs, 2H), 4.49-4.33 (m, 2H), 4.32-4.17 (m, 3H), 4.05 (brs, 1H), 3.55 (brs, 3H), 2.20 (brs, 2H), 2.00-1.05 (m, 18H).

***N*-cyclohexyl-*N*-(cyclohexylcarbamoyl)-1,2,5,6-tetrahydropyridine-3-carboxamide (2k). 1k** (24.4 mg, 0.0439 mmol) was dissolved in ACN (3 mL), diethylamine (300 µL, 2.91 mmol) was added and the reaction mixture was stirred for 3 h at 20 °C. The reaction mixture was evaporated to about 1 mL and

the product was isolated by preparative TLC (DCM:MeOH = 12:1; R_f = 0.06-0.22) and appeared as slightly yellowish oil (12.5 mg, 85%).

^{1}H-NMR (400MHz, $CDCl_3$) δ 6.74 (d, *J*=7.5Hz, 1H, CONH), 6.21 (m, 1H, H-4), 4.02 (m, 1H, Cy1 H-1), 3.62 (m, 1H, Cy2 H-1), 3.58 (m, 2H, H-2), 2.97 (t, *J*=5.8Hz, 2H, H-6), 2.17 (m, 2H, H-5), 1.95 (m, 2H, Cy1 H-2a,6a), 1.90 (m, 2H, Cy2 H-2a,6a), 1.79 (m, 2H, Cy1 H-3a,5a), 1.75 (m, 2H, Cy1 H-2b,6b), 1.70 (m, 2H, Cy2 H-3a,5a), 1.61 (m, 2H, Cy1,2 H-4a), 1.35 (m, 2H, Cy2 H-3b,5b), 1.27 (m, 2H, Cy1 H-3b,5b), 1.18 (m, 2H, Cy2 H-2b,6b), 1.17 (m, 2H, Cy1,2 H-4b).* ^{13}C-NMR (100MHz, $CDCl_3$) δ 171.1 (C=O), 154.2 (NCON), 135.6 (C-3), 128.0 (C-4), 57.0 (Cy1 C-1), 49.8 (Cy2 C-1), 44.4 (C-2), 41.8 (C-6), 32.7 (Cy2 C-2,6), 30.9 (Cy1 C-2,6), 26.3 (Cy1 C-3,5), 25.4 (Cy1 C-4), 25.3 (Cy2 C-4), 24.7 (Cy2 C-3,5), 24.6 (C-5). ^{15}N-NMR (41MHz, $CDCl_3$) δ -256.7 (CONHCy2).** HRMS (ESI) calcd for $C_{19}H_{32}N_3O_2$ ($M + H^+$) 334.2489, found 334.2492. *The guvacoline ^{1}H NH signal could not be found. ** The guvacoline and imide ^{15}N signals could not be found.

sodium diphenylmethanolate. Diphenylmethanol (300 mg, 1.62 mmol) was dissolved in dry THF (10 mL) and sodium (100 mg, 4.35 mmol) was added. The mixture was slightly heated until the gas evolution stopped. Excessive sodium was removed and the suspension was concentrated under reduced pressure. The waxy residue was dissolved in dry DMF (3.35 mL) and used for the synthesis of **3b** and **7** without characterization. **sodium 4,4'-difluordiphenylmethanolate**, **sodium 4,4'-dimethoxydiphenylmethanolate**, **sodium (4-bromophenyl)(4-fluorophenyl)methanolate**, **bis(6-fluoropyridin-3-yl)methanolate** and **furan-2-yl(phenyl)methanolate** were prepared accordingly.

benzhydryl 1-methyl-1,2,5,6-tetrahydropyridine-3-carboxylate (3b). Arecaidine (20.0 mg, 0.142 mmol) was suspended in dry DMF (2 mL) and heated gently until almost everything dissolved. CDI (23.0 mg, 0.142 mmol) was added as solid. After 15 min sodium diphenylmethanolate (0.59 mL of a 0.1 g/mL solution, 0.284 mmol) was added and the reaction mixture was stirred for 18 h at 20 °C.

The reaction mixture was poured on water (10 mL) and extracted with DCM (3x 10 mL). The organic phase was concentrated under reduced pressure and purified by preparative TLC (EE; R_f = 0.29-0.50). The product was obtained as colorless oil (8.3 mg, 19 %).

^{1}H-NMR (400MHz, $CDCl_3$) δ 7.34 (m, 8H, Ph H-2,3,5,6), 7.28 (m, 2H, Ph H-4), 7.15 (m, 1H, H-4), 6.94 (s, $CHPh_2$), 3.21 (m, 2H, H-2), 2.51 (t, *J*=5.6Hz, 2H, H-6), 2.40 (m, 2H, H-5), 2.42 (s, 3H, NCH_3). ^{13}C-NMR (100MHz, $CDCl_3$) δ 164.7 (C=O), 140.3 (Ph C-1), 138.3 (C-4), 129.1 (C-3), 128.5 (Ph C-3,5), 127.8 (Ph C-4), 127.1 (Ph C-2,6), 53.2 (C-2), 50.8 (C-6), 45.8 (NCH_3), 26.8 (C-5). ^{15}N-NMR (41MHz, $CDCl_3$) δ -349.7 (NCH_3). HRMS (ESI) calcd for $C_{20}H_{22}NO_2$ ($M + H^+$) 308.1645, found 308.1656.

bis(4-fluorophenyl)methyl 1-methyl-1,2,5,6-tetrahydropyridine-3-carboxylate (3c). Arecaidine (20.0 mg, 0.142 mmol) was suspended in dry DMF (3 mL) and heated gently until almost everything dissolved. CDI (23.0 mg, 0.142 mmol) was added as solid. After 1 h sodium 4,4'-difluordiphenylmethanolate (0.69 mL of a 0.1 g/mL solution, 0.284 mmol) was added and the reaction mixture was stirred for 60 h at 20 °C. The reaction mixture was poured on water (10 mL) and extracted with EE (2x 20 mL). The organic phase was washed with water (10 mL), dried over Na_2SO_4, concentrated under reduced pressure and purified by preparative TLC (EE; R_f = 0.18-0.45). The product was obtained as colorless oil (4.4 mg, 9 %).

^{1}H-NMR (600MHz, $CDCl_3$) δ 7.28 (m, 4H, Ph H-3,5), 7.14 (m, 1H, H-4), 7.03 (m, 4H, Ph H-2,6), 6.90 (s, 1H, $CHPh_2$), 3.22 (m, 2H, H-2), 2.54 (t, *J*=5.6Hz, 2H, H-6), 2.44 (s, 3H, NCH_3), 2.43 (m, 2H, H-5). ^{13}C-NMR (151MHz, $CDCl_3$) δ 164.6 (C=O), 162.5 (d, *J*=247.0Hz, Ph C-4), 138.7 (C-4), 136.0 (d, *J*=3.0Hz, Ph C-1), 129.0 (d, *J*=8.3Hz, Ph C-2,6), 128.8 (C-3), 115.6 (d, *J*=22.1Hz, Ph C-3,5), 75.6 ($CHPh_2$), 53.1 (C-2), 50.8 (C-6), 45.7 (NCH_3), 26.7 (C-5). HRMS (ESI) calcd for $C_{20}H_{20}F_2NO_2$ ($M + H^+$) 344.1457, found 344.1462.

bis(4-methoxyphenyl)methyl 1-methyl-1,2,5,6-tetrahydropyridine-3-carboxylate (3d). Arecaidine (30.0 mg, 0.213 mmol) was suspended in dry DMF (4 mL) and heated gently until almost everything dissolved. CDI (34.5 mg, 0.213 mmol) was added as solid. After 1 h sodium 4,4'-dimethoxydiphenylmethanolate (1.13 mL of a 0.1 g/mL solution, 0.426 mmol) was added and the reaction mixture was stirred for 24 h at 20 °C. The reaction mixture was poured on water (10 mL) and extracted with EE (2x 20 mL). The organic phase was washed with water (10 mL), dried over Na_2SO_4, concentrated under reduced pressure and purified by preparative TLC (EE; R_f = 0.18-0.45). The product was obtained as colorless oil (2.8 mg, 4 %).

^{1}H-NMR (400MHz, $CDCl_3$) δ 7.24 (m, 4H, Ph H-2,6), 7.11 (m, 1H, H-4), 6.88 (s, 1H, $CHPh_2$), 6.86 (m, 4H, Ph H-3,5), 3.79 (s, 6H, OCH_3), 3.20 (m, 2H, H-2), 2.51 (t, *J*=5.7Hz, 2H, H-6), 2.41 (s, 3H, NCH_3), 2.38 (m, 2H, H-5). ^{13}C-NMR (100MHz, $CDCl_3$) δ 164.8 (C=O), 159.1 (Ph C-4), 138.0 (C-4), 132.7 (Ph C-1), 129.1 (C-3), 128.4 (Ph C-2,6), 113.8 (Ph C-3,5), 76.2 ($CHPh_2$), 53.1 (C-2), 50.7 (C-6), 45.7 (NCH_3), 26.6 (C-5). HRMS (ESI) calcd for $C_{20}H_{26}NO_4$ ($M + H^+$) 368.1856, found 368.1855.

(4-bromophenyl)(4-fluorophenyl)methyl 1-methyl-1,2,5,6-tetrahydropyridine-3-carboxylate (3e). Arecaidine (40.0 mg, 0.284 mmol) was suspended in dry DMF (5 mL) and heated gently until almost everything dissolved. CDI (46.1 mg, 0.284 mmol) was added as solid. After 30 min sodium (4-bromophenyl)(4-fluorophenyl)methanolate (1.72 mL of a 0.1 g/mL solution, 0.568 mmol) was added and the reaction mixture was stirred for 2 weeks at 20 °C. The reaction mixture was poured on water (15 mL) and extracted with EE (2x 25 mL). The organic phase was washed with water (10 mL), dried over Na_2SO_4, concentrated under reduced pressure and purified by preparative TLC (EE; R_f = 0.28-0.42). The product was obtained as slightly yellow oil (28.4 mg, 25 %).

^{1}H-NMR (400MHz, $CDCl_3$) δ 7.46 (m, 2H, Ph-Br H-3,5), 7.28 (m, 2H, Ph-F H-2,6), 7.19 (m, 2H, Ph-Br H-2,6), 7.13 (m, 1H, H-4), 7.02 (m, 2H, Ph-F H-3,5), 6.86 (s, 1H, $CHPh_2$), 3.18 (m, 2H, H-2), 2.51 (t, *J*=5.6Hz, 2H, H-6), 2.41 (s, 3H, NCH_3), 2.40 (m, 2H, H-5). ^{13}C-NMR (100MHz, $CDCl_3$) δ 164.4 (C=O),

162.4 (d, *J*=247.2Hz, Ph-F C-4), 139.1 (Ph-Br C-1), 138.7 (C-4), 135.6 (d, *J*=3.2Hz, Ph-F C-1), 131.7 (Ph-Br C-3,5), 128.9 (d, *J*=8.3Hz, Ph-F C-2,6), 128.6 (Ph-Br C-2,6), 122.0 (Ph-Br C-4), 115.5 (d, *J*=21.6Hz, Ph-F C-3,5), 75.4 ($CHPh_2$), 53.1 (C-2), 50.7 (C-6), 45.7 (NCH_3), 26.7 (C-5). ^{19}F-NMR (377MHz, $CDCl_3$) δ -113.7 (m). ^{15}N-NMR (41MHz, $CDCl_3$) δ -349.8 (NCH_3). HRMS (ESI) calcd for $C_{20}H_{20}BrFNO_2$ (M + H^+) 404.0656, found 404.0668.

The racemic product was resolved on an AGP 0.3cmØ×5cm 5µM column using 12 % 2-propanol in 10 mM NH_4Ac pH 5.8 at a flow of 0.5 mL/min (Figure S5, Supporting Information). 2 µL of a 10 mg/mL solution in 2-propanol was injected 10 times resulting in baseline separation of the enantiomers. The pooled fractions were diluted with the same amount of water, subjected to solid phase extraction and eluted with ethanol (10 mL). Using a PerkinElmer 341 polarimeter with a 1 dm cell, (-) was assigned to the enantiomer with the stronger interaction to the stationary phase and (+) was assigned to the enantiomer with the weaker interaction to the stationary phase.

bis(6-fluoropyridin-3-yl)methanol. Mg turnings (345 mg, 14.2 mmol) were stirred in dry THF (10 mL) and activated with $BrCH_2CH_2Br$ (two drops). 5-bromo-2-fluoropyridine (500 mg, 2.84 mmol) in dry THF (2 mL) was added dropwise at 20 °C and the reaction mixture was refluxed for 45 min. Ethyl formate (115 µL, 1.42 mmol) in Et_2O (3 mL) was added dropwise at 20 °C and the reaction mixture was stirred for further 30 min. The reaction mixture was poured on sat. aq. NH_4Cl (20 mL) and extracted with EE (3x 15 mL) The combined organic phases were dried with Na_2SO_4 and evaporated. Preparative TLC (EE, R_f = 0.18-0.33, when developed twice) afforded the product (54 mg, 17 %) as yellow wax.

^{1}H-NMR (200MHz, $CDCl_3$) δ 8.21 (m, 2H, H-2), 7.76 (m, 2H, H-4), 6.93 (m, 2H, H-5), 5.95 (s, 1H, $CHPyr_2$), 3.18 (brs, 1H, OH). ^{13}C-NMR (50MHz, $CDCl_3$) δ 163.4 (d, *J*=240.8Hz, C-6), 145.9 (d, *J*=15.0Hz, C-2), 139.8 (d, *J*=8.2Hz, C-4), 136.3 (d, *J*=4.6Hz, C-3), 110.0 (d, *J*=37.4Hz, C-5), 70.7 ($CHPyr_2$). HRMS (ESI) calcd for $C_{11}H_8F_2N_2NaO$ (M + Na^+) 245.0495, found 245.0497.

bis(6-fluoropyridin-3-yl)methyl 1-methyl-1,2,5,6-tetrahydropyridine-3-carboxylate (3f). Arecaidine (30.0 mg, 0.213 mmol) was suspended in dry DMF (4 mL) and heated gently until almost everything dissolved. CDI (34.5 mg, 0.213 mmol) was added as solid. After 1 h sodium bis(6-fluoropyridin-3-yl)methanolate (1.04 mL of a 0.1 g/mL solution, 0.426 mmol) was added and the reaction mixture was stirred for 24 h at 20 °C. The reaction mixture was poured on water (15 mL) and extracted with EE (3x 15 mL). The organic phase was washed with water (10 mL), dried over Na_2SO_4, concentrated under reduced pressure and purified by preparative TLC (EE; R_f = 0.08-0.10) as well as preparative TLC on alox (PE:EE=2:1), yielding the product as colorless oil (1.8 mg, 3 %).

^{1}H-NMR (500MHz, $CDCl_3$) δ 8.24 (m, 2H, Pyr H-2), 7.74 (m, 2H, Pyr H-4), 7.32 (m, 1H, H-4), 7.00 (s, 1H, $CHPyr_2$), 6.99 (m, 2H, Pyr H-6), 4.21 (m, 1H, H-2), 3.54 (m, 1H, H-6) 3.48 (m, 1H, H-2), 3.32 (m, 1H, H-5), 2.92 (s, 3H, NCH_3), 2.91 (m, 1H, H-6), 2.58 (m, 1H, H-5). ^{13}C-NMR (125MHz, $CDCl_3$) δ 163.63 (d, *J*=240.5Hz, Pyr C-6), 163.59 (d, *J*=240.5Hz, Pyr C-6), 162.1 (C=O), 146.7 (d, *J*=7.7Hz, Pyr C-2), 146.6 (d, *J*=7.7Hz, Pyr C-2), 140.17 (d, *J*=7.5Hz, Pyr C-4), 138.6 (C-4), 131.8 (d, *J*=4.6Hz, Pyr C-3), 131.5 (d, *J*=4.6Hz, Pyr C-3), 123.2 (C-3), 110.3 (d, *J*=37.4Hz, Pyr C-5), 110.2 (d, *J*=37.4Hz, Pyr C-5), 72.5 ($CHPyr_2$), 50.3 (C-2), 49.3 (C-6), 43.2 (NCH_3), 23.1 (C-5). ^{19}F-NMR (471MHz, $CDCl_3$) δ -66.6 (ddd, *J*=17.1Hz, *J*=7.0Hz, *J*=2.3Hz). HRMS (ESI) calcd for $C_{18}H_{18}F_2N_3O_2$ ($M + H^+$) 346.1362, found 346.1366.

furan-2-yl(phenyl)methyl 1-methyl-1,2,5,6-tetrahydropyridine-3-carboxylate (3g). Arecaidine (40.0 mg, 0.284 mmol) was suspended in dry DMF (5 mL) and heated gently until almost everything dissolved. CDI (46.1 mg, 0.284 mmol) was added as solid. After 20 min sodium furan-2-yl(phenyl)methanolate (1.11 mL of a 0.1 g/mL solution, 0.568 mmol) was added and the reaction mixture was stirred for 60 h at 20 °C. The crude reaction mixture was purified by semipreparative HPLC with Two injections of 1.5 mL each were performed and the product fractions were immediately collected on DCM. The combined organic phases were dried with brine and $MgSO_4$,

filtered and evaporated, yielding the product as a yellowish oil (6 mg, 15 %). This work-up procedure was chosen due to the observed instability of this compound on silica and alox stationary phases. The isolated compound was sufficiently stable for chemical characterization. Despite storage at -20 °C, HPLC analysis prior to planned affinity measurements revealed inacceptable decomposition, excluding it from further evaluation.

^{1}H-NMR (400MHz, $CDCl_3$) δ 7.43 (m, 2H, Ph H-2,6), 7.40 (m, 1H, Fur H-5), 7.37 (m, 2H, Ph H-3,5), 7.35 (m, 1H, Ph H-4), 7.12 (m, 1H, H-4), 6.96 (s, 1H, CHPhFur), 6.31 (dd, *J*=3.3Hz, *J*=1.9Hz, 1H, Fur H-4), 6.19 (d, *J*=3.3Hz, 1H, Fur H-3), 3.19 (m, 2H, H-2), 2.50 (m, 2H, H-6), 2.41 (s, 3H, NCH_3), 2.38 (m, 2H, H-5). ^{13}C-NMR (100MHz, $CDCl_3$) δ 164.5 (C=O), 152.4 (Fur C-2), 143.2 (Fur C-5), 138.5 (C-4), 137.5 (Ph C-1), 128.8 (C-3), 128.5 (Ph C-3,5), 128.3 (Ph C-4), 127.1 (Ph C-2,6), 70.3 (CHPhFur), 53.1 (C-6), 50.7 (C-6), 45.7 (NCH_3), 26.6 (C-5). ^{15}N-NMR (41MHz, $CDCl_3$) δ -349.5 (NCH_3). HRMS (ESI) calcd for $C_{18}H_{20}NO_3$ ($M + H^+$) 298.1438, found 298.1433.

2-oxo-1,2-diphenylethyl 1-methyl-1,2,5,6-tetrahydropyridine-3-carboxylate (3h). Arecaidine (40.0 mg, 0.284 mmol) was suspended in dry DMF (5 mL) and heated gently until almost everything dissolved. CDI (46.1 mg, 0.284 mmol) was added as solid. After 1 h (±)-benzoin (121 mg, 0.568 mmol) was added and the reaction mixture was stirred for 5 days at 20 °C. The reaction mixture was poured on water (15 mL) and extracted with EE (3x 15 mL). The combined organic phases were dried over Na_2SO_4 and concentrated under reduced pressure. Half of the resulting residue was purified by preparative TLC (EE; R_f = 0.17-0.40), yielding the product as colorless oil (12.0 mg, 3 %).

^{1}H-NMR (400MHz, $CDCl_3$) δ 7.95 (m, 2H, COPh H-2,6), 7.51 (m, 1H, COPh H-4), 7.48 (m, 2H, Ph H-2,6), 7.40 (m, 2H, COPh H-3,5), 7.37 (m, 1H, Ph H-4), 7.35 (m, 2H, Ph H-3,5), 7.17 (m, 1H, H-4), 6.91 (s, 3H, CHPh), 3.20 (m, 2H, H-2), 2.52 (m, 2H, H-6), 2.41 (s, 3H, NCH_3), 2.40 (m, 2H, H-5). ^{13}C-NMR (100MHz, $CDCl_3$) δ 193.9 (COPh), 165.0 (COO), 139.2 (C-4), 134.7 (COPh C-1), 133.8 (Ph C-1), 133.4 (COPh C-4), 129.2 (Ph C-4), 129.1 (Ph C-3,5), 128.8 (COPh C-2,6), 128.62 (COPh C-3,5), 128.56 (Ph C-2,6), 128.2 (C-

3), 77.3 (CHPh), 52.9 (C-2), 50.6 (C-6), 45.6 (NCH_3), 26.6 (C-5). HRMS (ESI) calcd for $C_{21}H_{22}NO_3$ ($M + H^+$) 336.1594, found 336.1600.

***N*-benzhydryl-1-methyl-1,2,5,6-tetrahydropyridine-3-carboxamide (3i).** Arecaidine (20.0 mg, 0.142 mmol) was suspended in dry DMF (3 mL) and heated gently until almost everything dissolved. CDI (23.0 mg, 0.142 mmol) was added as solid. After 1 h benzhydrylamine (52.0 mg, 0.284 mmol) was added and the reaction mixture was stirred for 18 h at 20 °C. DMF was evaporated under reduced pressure and the residue was purified by preparative TLC (DCM:MeOH = 20:1; R_f = 0.36-0.47 when developed twice; subsequently: DCM:MeOH = 30:1, analytical TLC plate, R_f = 0.11-0.27). The product was obtained as colorless oil (5.3 mg, 12 %).

^{1}H-NMR (400MHz, $CDCl_3$) δ 7.33 (m, 4H, Ph H-3,5), 7.27 (m, 2H, Ph H-4), 7.23 (m, 4H, Ph H-2,6) ,6.56 (m, 1H, H-4), 6.28 (m, 2H, $CHPh_2$, NH), 3.26 (m, 2H, H-2), 2.57 (t, *J*=5.7Hz, 2H, H-6), 2.44 (s, 3H, NCH_3), 2.38 (m, 2H, H-5). ^{13}C-NMR (100MHz, $CDCl_3$) δ 165.8 (C=O), 141.4 (Ph C-1), 132.4 (C-3), 130.1 (C-4), 128.7 (Ph C-3,5), 127.5 (Ph C-4), 127.4 (Ph C-2,6), 56.9 ($CHPh_2$), 53.2 (C-2), 50.8 (C-6), 45.5 (NCH_3), 25.8 (C-5). ^{15}N-NMR (41MHz, $CDCl_3$) δ -260.3 (CONH), -348.9 (NCH_3). HRMS (ESI) calcd for $C_{20}H_{22}N_2NaO$ ($M + Na^+$) 329.1624, found 329.1634.

2-[2-(2-methoxyethoxy)ethoxy]ethyl 1-methyl-1,2,5,6-tetrahydropyridine-3-carboxylate (3j). Arecaidine (20.0 mg, 0.142 mmol) was suspended in dry DMF (2 mL) and CDI (23.0 mg, 0.142 mmol) was added as solid. The suspension was gently heated until a solution was obtained. Triethylene glycol monomethyl ether (50 µL, 0.312 mmol) was added and the reaction mixture was stirred for 60 h at rt. The solvent was evaporated and the residue was purified by preparative TLC (PE:EE = 2:1; R_f = 0.22-0.38). The product was obtained as colorless oil (7.2 mg, 18 %).

^{1}H-NMR (400MHz, $CDCl_3$) δ 7.03 (m, 1H, H-4), 4.29 (m, 2H, TEG H-1), 3.73 (m, 2H, TEG H-2), 3.66 (m, 4H, TEG H-3,4), 3.65 (m, 2H, TEG H-5), 3.55 (m, 2H, TEG H-6), 3.38 (s, 3H, OCH_3), 3.17 (m, 2H, H-2),

2.52 (t, *J*=5.6Hz, 2H, H-6), 2.42 (s, 3H, NCH_3), 2.38 (m, 2H, H-5). ^{13}C-NMR (100MHz, $CDCl_3$) δ 165.6 (C=O), 137.8 (C-4), 128.7 (C-3), 71.9 (TEG C-6), 70.62 (TEG C-3)*, 70.61 (TEG C-4)*, 70.58 (TEG C-5)*, 69.2 (TEG C-2), 63.6 (TEG C-1), 59.0 (OCH_3), 53.1 (C-2), 50.7 (C-6), 45.6 (NCH_3), 26.5 (C-5). ^{15}N-NMR (41MHz, $CDCl_3$) δ -349.7 (NCH_3). HRMS (ESI) calcd for $C_{14}H_{26}NO_5$ ($M + H^+$) 288.1805, found 288.1815. *indistinguishable

_N_-cyclohexyl-_N_-(cyclohexylcarbamoyl)-1-methyl-1,2,5,6-tetrahydropyridine-3-carboxamide (3k). Arecaidine (30.0 mg, 0.213 mmol) and diphenylmethanol (78.3 mg, 0.425 mmol) were suspended in dry DMF (1.5 mL) and dry DCM (0.5 mL). DMAP (3 mg, 0.025 mmol) was added at 20 °C and the reaction mixture was cooled to 0 °C. DCC (48.2 mg, 0.234 mmol) was added as solution in DMF (0.5 mL) and the reaction mixture was stirred at 0 °C for 10 min, at 20 °C for 40 min and at 70°C for 30 min. The solvent was evaporated and the residue was purified by preparative TLC (DCM:MeOH = 11:1; R_f = 0.20-0.50). The product was obtained as off-white solid (50.9 mg, 69 %). Crystals suitable for single-crystal X-ray crystallography were grown from $CDCl_3$/hexane by slow evaporation of solvents. Crystallographic analysis is described in the Supporting Information.

^{1}H-NMR (400MHz, $CDCl_3$) δ 6.77 (d, *J*=7.5Hz, 1H, NH), 6.15 (m, 1H, H-4), 4.01 (m, 1H, Cy1 H-1a), 3.63 (m, 1H, Cy2 H-1a), 3.13 (m, 2H, H-2), 2.51 (t, *J*=5.7Hz, 2H, H-6), 2.39 (s, 3H, NCH_3), 2.28 (m, 2H, H-5), 2.03 (m, 2H, Cy1 H-2a,6a), 1.91 (m, 2H, Cy2 H-2a,6a), 1.78 (m, 2H, Cy1 H-3a,5a), 1.73 (m, 2H, Cy1 H-2b,6b), 1.69 (m, 2H, Cy2 H-3a,5a), 1.60 (m, 2H, Cy1,2 H-4a), 1.35 (m, 2H, Cy2 H-3b,5b), 1.27 (m, 2H, Cy1 H-3b,5b), 1.17 (m, 4H, Cy1,2 H-4b, Cy2 H-2b,6b). ^{13}C-NMR (100MHz, $CDCl_3$) δ 171.5 (C=O), 154.3 (NCON), 134.3 (C-3), 127.6 (C-4), 57.7 (Cy1 C-1), 54.1 (C-2), 50.9 (C-6), 49.6 (Cy2 C-1), 45.6 (NCH_3), 32.7 (Cy2 C-2,6), 30.9 (Cy1 C-2,6), 26.3 (Cy1 C-3,5), 25.54 (C-5), 25.47 (Cy1 C-4)*, 25.3 (Cy2 C-4)*, 24.7 (Cy2 C-3,5). ^{15}N-NMR (41MHz, $CDCl_3$) δ -350.7 (NCH_3). HRMS (ESI) calcd for $C_{20}H_{34}N_3O_2$ ($M + H^+$) 348.2646, found 348.2654. *indistinguishable

Note: The initial intention of this reaction was the synthesis of **3b**, however, the *N*-acylurea was isolated under the given conditions. For the synthesis of **3k** the addition of diphenylmethanol can be omitted.

2-oxo-2-(6-oxo-5,6-dihydro-11*H*-benzo[*e*]pyrido[3,2-*b*][1,4]diazepin-11-yl)ethyl 1-methyl-1,2,5,6-tetrahydropyridine-3-carboxylate (3l). Arecaidine (19.6 mg, 0.139 mmol) was suspended in dry DMF (3 mL) and heated gently until almost everything dissolved. NaH (8.3 mg of a 60 % dispersion, 0.208 mmol) was added and the mixture was stirred for 1 min. 11-(chloroacetyl)-5,11-dihydro-6*H*-pyrido[2,3-*b*][1,4]benzodiazepin-6-one (40.0 mg, 0.139 mmol) and NaI (20.8 mg, 0.139 mmol) was added and the mixture was heated to 70 °C for 1 h. DMF was evaporated *in vacuo*, the residue was suspended in DCM and filtered. The product was isolated from the filtrate by preparative TLC (DCM:MeOH = 12:1; R_f = 0.19-0.38) and appeared as white solid (6.9 mg, 13 %). ^{1}H-NMR (600MHz, $CDCl_3$) δ 9.74 (brs, 1H, CONH), 8.31 (brs, 1H, Ar H-2), 7.96 (d, *J*=7.7Hz, 1H, Ar H-7), 7.63 (m, 2H, Ar H-9,10), 7.62 (dd, *J*=7.9Hz, *J*=1.6Hz, 1H, Ar H-4), 7.43 (m, 1H, Ar H-8), 7.33 (dd, *J*=7.9Hz, *J*=4.8Hz, 1H, Ar H-3), 6.88 (m, 1H, H-4), 5.02 (m, 1H, $COCH_2$), 4.71 (d, *J*=12.5Hz, 1H, $COCH_2$), 3.20 (d, *J*=16.2Hz, 1H, H-2), 3.02 (d, *J*=16.2Hz, 1H, H-2), 2.55 (m, 1H, H-6), 2.45 (m, 1H, H-6), 2.39 (s, 3H, NCH_3), 2.35 (m, 2H, H-5). ^{13}C-NMR (151MHz, $CDCl_3$) δ 167.6 (NHCO), 166.8 (NCO), 164.7 (COO), 145.6 (Ar C-11a), 145.3 (Ar C-2), 140.3 (Ar C-10a), 139.0 (C-4), 133.5 (Ar C-9), 131.5 (Ar C-7), 130.9 (Ar C-4a), 130.6 (Ar C-4), 128.4 (Ar C-8,10), 127.9 (C-3), 124.7 (Ar C-3), 62.8 (CH_2O), 52.9 (C-2), 50.7 (C-6), 45.6 (NCH_3), 26.5 (C-5).* HRMS (ESI) calcd for $C_{21}H_{21}N_4O_4$ ($M + H^+$) 393.1557, found 393.1563.

* one quaternary carbon (Ar C-6a) could not be found.

methyl 1-(2-oxo-2-(6-oxo-5,6-dihydro-11*H*-benzo[*e*]pyrido[3,2-*b*][1,4]diazepin-11-yl)ethyl)-1,2,5,6-tetrahydropyridine-3-carboxylate (3m). Guvacoline (9.0 mg, 0.0638 mmol) was dissolved in dry ACN (3 mL) and $NaHCO_3$ (5.4 mg, 0.0638 mmol) and 11-(chloroacetyl)-5,11-dihydro-6*H*-pyrido[2,3-

b][1,4]benzodiazepin-6-one (18.3 mg, 0.0638 mmol) were added. The reaction mixture was stirred for 20 min at 70 °C and for 60 h at 20 °C, filtered and purified by preparative TLC (EE; R_f = 0.16-0.32). The product was obtained as off-white solid (6.7 mg, 27 %).

^{1}H-NMR (400MHz, $CDCl_3$) δ 9.60 (brs, 1H, CONH), 8.29 (brs, 1H, Ar H-2), 7.96 (m, 1H, Ar H-7), 7.64 (m, 2H, Ar H-9,10), 7.55 (dd, *J*=7.9Hz, *J*=1.3Hz, 1H, Ar H-4), 7.44 (m, 1H, Ar H-8), 7.28 (dd, *J*=7.9Hz, *J*=4.7Hz, 1H, Ar H-3), 6.87 (m, 1H, H-4), 3.66 (m, 1H, $COCH_2$), 3.63 (s, 3H, OCH_3), 3.40 (d, *J*=15.0Hz, 1H, $COCH_2$), 3.18 (m, 1H, H-2), 2.94 (m, 1H, H-2), 2.56 (m, 1H, H-6), 2.36 (m, 1H, H-6), 2.20 (m, 1H, H-5), 2.05 (m, 1H, H-5). ^{13}C-NMR (151MHz, $CDCl_3$) δ 169.6 (NHCO), 168.0 (NCO), 166.0 (COO), 147.2 (Ar C-11a), 144.9 (Ar C-2), 140.7 (Ar C-10a), 137.5 (C-4), 133.4 (Ar C-9), 131.3 (Ar C-7), 130.6 (Ar C-4a), 129.8 (Ar C-4), 128.7 (Ar C-6a), 128.5 (Ar C-10), 128.1 (Ar C-8), 123.9 (Ar C-3), 60.3 ($COCH_2$), 51.5 (OCH_3), 50.8 (C-2), 48.3 (C-6), 26.3 (C-5). HRMS (ESI) calcd for $C_{21}H_{21}N_4O_4$ ($M + H^+$) 393.1557, found 393.1565.

4-methylmorpholine-2-carbonitrile (4). A solution of 2-chloroacrylonitrile (1.37 mL, 17.1 mmol) in dry THF (3 mL) was added to a stirred solution of *N*-methylethanolamine (1.38 mL, 17.1 mmol) in dry THF (3 mL). After 40 min the solution was cooled to 0 °C and KO^tBu (1.92 g, 17.1 mmol) was added in portions. The reaction mixture was stirred for 10 min on ice, before THF was removed under reduced pressure. The crude product was purified by Kugelrohr distillation to yield a colorless liquid (1.24 g, 57 %).

^{1}H-NMR (400MHz, $CDCl_3$) δ 4.59 (m, 1H, H-2), 4.00 (m, 1H, H-6), 3.75 (m, 1H, H-6), 2.70 (m, 1H, H-3), 2.56 (m, 1H, H-5), 2.52 (m, 1H, H-3), 2.32 (m, 1H, H-5), 2.31 (s, 3H, NCH_3). ^{13}C-NMR (151MHz, $CDCl_3$) 117.1 (CN), 65.0 (C-6), 64.2 (C-2), 56.6 (C-3), 54.1 (C-5), 46.0 (NCH_3). HRMS (ESI) calcd for $C_6H_{11}N_2O$ ($M + H^+$) 127.0866, found 127.0869.

2-carboxy-4-methylmorpholin-4-ium bromide (5). 4 (1.24 g, 9.83 mmol) was refluxed in H_2O (6 mL) containing 48 % aq. HBr solution (6 mL) for 1.5 h. The reaction mixture was evaporated to dryness. The product was separated from NH_4Br by fractional crystallization from H_2O and drying in high vacuum at 50 °C. The product appeared as white crystals (1.68 g, 76 %) suitable for single crystal X-ray crystallography.

^{1}H-NMR (400MHz, D_2O) 4.52 (m, 1H, H-2), 4.26 (m, 1H, H-6), 3.98 (m, 1H, H-3), 3.91 (m, 1H, H-6), 3.56 (m, 1H, H-5), 3.20 (m, 1H, H-5), 3.19 (m, 1H, H-3), 2.99 (s, 3H, NCH_3). ^{13}C-NMR (151MHz, D_2O) 171.1 (COOH), 72.8 (C-2), 64.3 (C-6), 54.3 (C-3), 53.1 (C-5), 44.2 (NCH_3). HRMS (ESI) calcd for $C_6H_{12}NO_3$ (M + H^+) 146.0812, found 146.0815.

***N*-benzhydryl-4-methylmorpholine-2-carboxamide (6). 4** (100 mg, 0.793 mmol) and diphenylmethanol (146 mg, 0.793 mmol) were stirred in formic acid (2 mL) at 90 °C for 5 days. The reaction mixture was cooled to 20 °C, poured on water (15 mL) and extracted with DCM (3x10 mL). The organic phases were combined, dried with Na_2SO_4 and half of the total volume was subjected to preparative TLC (EE, R_f = 0.04-0.13). The product appeared as off-white, crystalline solid (13 mg, 11 %).

^{1}H-NMR (400MHz, $CDCl_3$) δ 7.33 (m, 4H, Ph H-3,5), 7.27 (m, 2H, Ph H-4), 7.23 (m, 4H, Ph H-2,6), 7.19 (brd, *J*=8.5Hz, 1H, CONH), 6.25 (d, *J*=8.5Hz, 1H, $CHPh_2$), 4.14 (dd, *J*=10.7Hz, *J*=2.7Hz, 1H, H-2), 3.94 (m, 1H, H-6), 3.75 (m, 1H, H-6), 3.24 (m, 1H, H-3), 2.71 (m, 1H, H-5), 2.34 (s, 3H, NCH_3), 2.17 (m, 1H, H-5), 2.01 (m, 1H, H-3). ^{13}C-NMR (100MHz, $CDCl_3$) δ 168.7 (CONH), 141.30 (Ph C-1), 141.28 (Ph C-1), 128.66 (Ph C-3,5), 128.64 (Ph C-3,5), 127.50 (Ph C-4), 127.44 (Ph C-2,6), 127.42 (Ph C-4), 127.26 (Ph C-2,6), 75.2 (C-2), 66.3 (C-6), 56.9 (C-3), 56.1 ($CHPh_2$), 54.2 (C-5), 45.8 (NCH_3). ^{15}N-NMR (41MHz, $CDCl_3$) δ -259.3 (CONH), -345.7 (NCH_3). HRMS (ESI) calcd for $C_{19}H_{23}N_2O_2$ (M + H^+) 311.1754, found 311.1759.

benzhydryl 4-methylmorpholine-2-carboxylate (7). 5 (80.0 mg, 0.354 mmol) was suspended in dry DMF (3 mL) and heated gently until almost everything dissolved. CDI (86.1 mg, 0.531 mmol) was added as solid. After 30 min sodium diphenylmethanolate (2.2 mL of a 0.1 g/mL solution, 1.06 mmol) was added and the reaction mixture was stirred for 18 h at 20 °C. The reaction mixture was poured on water (30 mL) and extracted with EE (3x 15 mL). The organic phase was concentrated under reduced pressure and half of it was purified by preparative TLC (PE:EE = 1:1; R_f = 0.16-0.35). The product was obtained as colorless oil (13.0 mg, 24 %).

^{1}H-NMR (400MHz, $CDCl_3$) δ 7.34 (m, 4H, Ph H-2,6), 7.33 (m, 4H, Ph H-3,5), 7.29 (m, 2H, Ph H-4), 6.98 (s, 1H, $CHPh_2$), 4.31 (dd, *J*=8.9Hz, *J*=2.9Hz, 1H, H-2), 4.03 (m, 1H, H-6), 3.70 (m, 1H, H-6), 2.95 (m, 1H, H-3), 2.55 (m, 1H, H-5), 2.34 (m, 1H, H-3), 2.31 (s, 3H, NCH_3), 2.26 (m, 1H, H-5). ^{13}C-NMR (100MHz, $CDCl_3$) δ 169.0 (C=O), 139.7 (Ph C-1), 139.6 (Ph C-1), 128.5 (Ph C-3,5), 128.03 (Ph C-4), 127.97 (Ph C-4), 127.2 (Ph C-2,6), 127.0 (Ph C-2,6), 77.3 ($CHPh_2$), 74.4 (C-2), 66.1 (C-6), 56.4 (C-3), 54.3 (C-5), 46.2 (NCH_3). ^{15}N-NMR (41MHz, $CDCl_3$) δ -347.2 (NCH_3). HRMS (ESI) calcd for $C_{19}H_{22}NO_3$ ($M + H^+$) 312.1594, found 312.1589.

1-(4-methylmorpholin-2-yl)-2-phenylethan-1-one (8). Mg turnings (116 mg, 4.76 mmol) were stirred in dry Et_2O (2 mL) and activated with $BrCH_2CH_2Br$ (two drops). Benzyl chloride (602 mg, 4.76 mmol) in dry Et_2O (3 mL) was added dropwise at 20 °C and the reaction mixture was stirred for 30 min. **4** (200 mg, 1.59 mmol) in Et_2O (3 mL) was added dropwise at 0 °C and the reaction mixture was stirred at room temperature for 1.5 h. The reaction was quenched with 1M aq. HCl (4 mL) and subsequently NaOH (0.5 g) was added. The resulting suspension was extracted with Et_2O (3x 10 mL) and combined organic phases were dried with Na_2SO_4 and evaporated. One third of the crude product was purified by preparative TLC (DCM:MeOH = 30:1; R_f = 0.22-0.61), yielding a yellowish oil (14 mg, 12 %).

^{1}H-NMR (400MHz, $CDCl_3$) δ 7.31 (m, 2H, Ph H-3,5), 7.25 (m, 1H, Ph H-4), 7.20 (m, 2H, Ph H-2,6), 4.07 (dd, *J*=10.3Hz, *J*=2.8Hz, 1H, H-2), 3.99 (m, 1H, H-6), 3.92 (d, *J*=16.0Hz, 1H, CH_2Ph), 3.87 (d, *J*=16.0Hz,

1H, CH_2Ph), 3.70 (m, 1H, H-6), 2.95 (m, 1H, H-3), 2.63 (m, 1H, H-5), 2.29 (s, 3H, NCH_3), 2.14 (m, 1H, H-5), 1.94 (m, 1H, H-3). ^{13}C-NMR (100MHz, $CDCl_3$) δ 206.6 (C=O), 133.6 (Ph C-1), 129.7 (Ph C-2,6), 128.5 (Ph C-3,5), 126.9 (Ph C-4), 80.1 (C-2), 66.7 (C-6), 56.0 (C-3), 54.5 (C-5), 46.2 (NCH_3), 45.2 (CH_2Ph). ^{15}N-NMR (41MHz, $CDCl_3$) δ -346.8 (NCH_3). HRMS (ESI) calcd for $C_{13}H_{18}NO_2$ ($M + H^+$) 220.1332, found 220.1337.

M1-M5 affinity determination

Membranes containing human M1, M2, M3, M4 or M5 receptors and CHO-K1 wild type membranes were prepared from the respective cell line according to a protocol adapted from Klotz *et al*.[48] Cells were grown to confluence in T175 flasks for membrane preparation. The medium was removed and the cell layer was washed with ice-cold PBS and suspended with a cell scraper in 2 mL/flask 10 mM Tris/HCl, 1 mM EDTA-buffer (pH 7.4) and 200 µL/flask of protease inhibitor. Cells were disrupted by passing the suspension through a G29 needle and the resulting homogenate was centrifuged (10 min, 1,000× *g*, 4 °C). The supernatant was again centrifuged (30 min, 100,000 g, 4 °C) and the resulting membrane pellet was suspended in 125 µL/flask 50 mM Tris/HCl-buffer (pH 7.4) and stored at -80 °C. In one batch typically ten T175 flasks were processed to membranes. The protein concentration of the membrane suspension was assessed with a photometric BCA assay and ranged from approx. 500-3000 µg/mL.

Stock solutions of compounds for affinity testing were prepared in DMSO and 50 mM Tris/HCl, 10 mM $MgCl_2$, 1 mM EDTA (pH 7.4) was used as assay buffer. The radioligand binding assay was performed in PP test tubes by mixing 5 µL of test compound in DMSO, 50 µL of [*N*-methyl-^{3}H]scopolamine methyl chloride in assay buffer and 445 µL of membrane suspension in assay buffer. 5 µL of 1 µM scopolamine was used instead of test compound to measure the nonspecific binding and 5 µL DMSO were used to assess the maximum binding potential. Effective concentrations of radioligand were 0.2 nM, 0.3 nM, 0.8 nM, 0.2 nM, 1 nM for M1-M5 and 4-30 µg membrane were

used per tube. After 1.5 h incubation at 23 °C the membrane bound radioactivity was recovered by filtration through GF/B glass fibre filters pre-soaked in 0.1 % PEI and measured in a β-counter.

At least five distinct concentrations of test compound (each pipetted in triplicate) were used to calculate the IC_{50} by a variable slope logistic regression in GraphPad Prism®. Inhibition constants (K_i) were calculated with the Cheng-Prusoff equation, with radioligand K_D values of 0.18 nM, 0.24 nM, 0.23 nM, 0.10 nM and 0.35 nM for M1-M5 as determined in the Supporting Information (Table S1). Results are given as average of at least three independent experiments.

EeAChE affinity and metabolism

Ellman's assay was performed according to a modified protocol from literature.[30] Briefly, 5 µL sample solution were pipetted in two columns of a flat bottom 96-well-plate and in the first two rows 5 µL water was used as a blank. Then 200 µL of the enzyme solution (0.0682 µg/mL) were added column after column. After 4 min, 48.8 µL of DTNB (0.5 mM) was added. After another minute for each row 48.8 µL of a different concentration of ATI (3 mM, 1.5 mM, 0.75 mM, 0.375 mM or 0.188 mM) was added. After two minutes the plate was placed in the photometric microplate reader, where the absorbance was measured in 10 s intervals for 10 min at 405 nm. For each sample concentration reciprocal ATI concentrations were plotted against the reciprocal slope of the kinetic measurement (sec/OD) and the resulting slope was plotted against the sample concentrations. The K_i was determined as the negative abscissa intercept of this plot. Graphs are depicted in the Supporting Information, Figure S6. Every sample was tested in three independent experiments. Sample solutions were prepared by prediluting 10 mM DMSO stock solutions of arecoline, **3b**-**m**, **6**-**8** and tacrine 1:10 in water to suppress the AChE inhibitory effect of DMSO.[49]

To study the EeAChE metabolism a solution containing the same concentration of the sample and the enzyme as used in the Ellman's Assay was prepared and incubated at 20 °C for 10 min and 60 min. For the blank water was used instead of enzyme solution. At the given timepoints the solution was

quenched with ACN:MeOH = 1:1 and analyzed by RP-HPLC. The sample peak area of the enzyme-containing solution and the blank was compared using a multiple comparisons 2way ANOVA.

Ligand docking

Ligand docking was performed in LigandScout 4.4_RC6 with a crystal structure of a human M1 mAChR bound to tiotropium[5] using AutoDock 4.2 with default settings. Protonated **3c** and tiotropium were docked to the orthosteric binding site and pharmacophores were generated to compare their interaction with the environment. **3c** features a calculated pKa of 7.99 (MarvinSketch 17.24) and therefore was docked in its protonated form to account for the expected higher abundance of this species under physiological conditions. The used sequence of crystal structure of the M1 receptor features also a small second chain. Mentioned residue numbers are suffixed with 'A' in order to be unambiguous and to stick with the PDB nomenclature.

Radiochemistry

For small scale reactions [^{11}C]CH_3I was trapped in 1.7 mL solvent. 200 µL of this solution were added to 1 mg of precursor in 200 µL solvent, whereat different solvents, reaction time and temperature were tested. The reaction mixture was quenched with 100 µL H_2O and analyzed with radio-HPLC. The non-isolated radiochemical yield[36] was determined by dividing the AUC of the product by the total AUC.

For automated syntheses [^{11}C]CH_3I was trapped in a reaction vessel containing 1 mg of precursor dissolved in 0.5 mL DMSO. The reaction mixture was heated to 80 °C for 2 min, cooled to 25 °C, quenched with 1 mL HPLC eluent and purified by preparative HPLC (conditions summarized in Table 7). The product fraction was collected in a stirred bulb containing 100 mL water. A solid phase extraction cartridge was used to isolate the product from the predominantly aqueous solution. The immobilized product was washed with 10 mL water, eluted with 1.5 mL ethanol and collected in a glass vial containing 6 mL sterile PBS. Subsequently, the cartridge was furthermore rinsed with 5 mL 0.9% NaCl solution to recover small amounts of remaining product.

Metabolic stability

15 µL microsomes were preincubated in 257 µL PBS, 15 µL solution A and 3 µL solution B by gently shaking at 37 °C for 10 min. 10 µL of tracer solution was added and 50 µL samples were taken at 0, 10, 20, 40 and 60 min. The samples were immediately quenched wit 50 µL ACN:MeOH = 1:1, centrifuged at 21,500 g for 5 min and 50 µL of the supernatant was analyzed with radio-HPLC. Peak areas of appearing radiometabolites were decay corrected for their retention times and related to the total peak area.

For metabolite identification a solution of **3b** in EtOH (10 mg/mL) was used instead of tracer solution. 50 mM NH_4Ac pH 9.3 was used as mobile phase to allow for HRMS measurement of the collected fraction.

Serum protein binding

5-20 µL tracer solution (depending on the activity concentration) was incubated with 1 mL human serum or 1 mL PBS for 50 min at 23 °C. Afterwards, 200 µL of the resulting mixture was pipetted on a filter and the total activity was measured prior filtration. Free tracer was separated from protein-bound tracer by ultrafiltration of 200 µL in Centrifree (2,100 g, 50 min) or Microcon (14,000 g, 40 min) filters. The amount of free tracer was determined from a measurement of a defined volume of the filtrate (usually 100 µL), which is corrected for time and to the theoretical total volume of 200 µL. The given ff% is corrected for nonspecific binding determined from the PBS measurement. Ultrafiltration of serum was performed in technical triplicates.

Kinetic studies using LigandTracer

Briefly, the LigandTracer system consists of a tilted, slowly rotating petridish containing medium with radioligand and locally seeded target cells. A radiodetector mounted above the upper part of the tilted dish measures the cell bound activity with every revolution and thus can follow the interaction kinetics between radioligand and cells in real-time.

One day before the experiment $1x10^6$ CHO-M1 cells were suspended in a volume of 1 mL medium and pipetted on an area of 1 cm^2 close to the edge of a petri dish. The cells were allowed to attach in the incubator overnight. 20 minutes prior to the measurement the medium was replaced with 3 mL FBS-free medium. The petri dish was placed on the LigandTracer device and a baseline measurement was started. In case of a preblocking experiment, this medium contained 10 µM scopolamine. The run was paused and carbon-11 labeled product solution was added *via* micropipette to reach the desired concentration and the run was continued until equilibrium was reached (detection time: 5 s, detection delay time: 0 s). A single petri dish was used to follow the interaction at up to three concentrations.

Direct radioligand binding assay using [^{11}C]3c

One day before the experiment CHO-M1 cells and wild type CHO cells were seeded to six-well plates ($2.5x10^5$ cells per well). The medium was removed and the cells were incubated with 0.3 nM, 3 nM or 30 nM [^{11}C]**3c** in FBS free medium containing 10 µM scopolamine, 10 µM pirenzepine or no competitor for 20 min at 20 °C. For the experiment at ≤ 4 °C the sixwell plates were put on ice 15 min prior to and during the incubation and the used incubation solutions were put on ice previously. The supernatant was removed and the cells were quickly washed with 3 mL icecold PBS. Cells were detached by shaking them for 10 min with 0.5 mL trypsin at 20 °C. The cell suspensions were transferred to PP test tubes and each well was rinsed with 1 mL medium. The tubes were measured in a gamma counter for 30 sec. The resulting count rate of the cell bound activity was corrected for decay and normalized to the incubation without competitor for each concentration. The experiment was performed in technical triplicates.

***In vitro* autoradiography**

Autoradiography was performed on sagittal mouse brain sections of two different individuals using [^{11}C]**3c** and [^{11}C]pirenzepine as a reference according to a previously published protocol described for [^{3}H]pirenzepine.[50] In brief, thawed and dried *cryo*-sections were pre-incubated in 50 mM KH_2PO_4

buffer (pH 7.4) following radioligand incubation for 40 min using the same buffer at 20 °C. Radioligand concentration was chosen with respect to affinity and molar activity (15 nM [^{11}C]pirenzepine; 3 nM and 30 nM [^{11}C]**3c**). Vicinal sections were co-incubated using 10 µM scopolamine or atropine as blocking agents. To remove unbound radioligand, sections were washed twice in ice-cold assay buffer for 5 min and dipped in ice-cold water. Dry sections were exposed to a phosphor screen in a lightproof cassette overnight. Stored radioactivity was read-out using a Cyclone Phosphor Imager and digital autoradiograms were generated using OptiQuant Software (Perkin Elmer).

Statistical analysis

All experiments were performed in at least three repetitions and values were expressed as mean ± standard deviation, if not stated otherwise. Statistical tests were performed with GraphPadPrism 6.

Supporting Information

Further syntheses of non-radioactive reference compounds supporting the formation of the desired [^{11}C]**3k** regioisomer; synthesis of [^{11}C]pirenzepine, chiral chromatogram of racemic **3e**; saturation binding of [^{3}H]NMS, details on EeAChE affinity testing; exemplary chromatogram of metabolic stability; metabolite identification; plasma stability; ^{1}H and ^{13}C NMR spectra; table of X-ray experimental parameters and crystal data of **3k** and **5** as well as illustration of the packing.

Corresponding Author Information

Verena Pichler: verena.pichler@meduniwien.ac.at

Author contributions

M.O. and V.P. designed the research concept, performed syntheses and compound characterization, performed preclinical experiments and analyzed the respective data and prepared the manuscript. K.P. performed preclinical experiments, analyzed data and proofread the manuscript. T.B. and C.V. designed and performed preclinical experiments, analyzed data and contributed to the manuscript.

A.R. performed and analyzed X-ray experiments and contributed to manuscript preparation. W.H. performed and analyzed NMR experiments and proofread the manuscript. H.S. contributed to compound design and syntheses concept and proofread the manuscript. M.M., W.W. and M.H. contributed to the overall research concept and preparation of the manuscript. All authors have given approval to the final version of the manuscript.

Funding

Funding was provided by the Medical University of Vienna and University of Vienna.

Declaration of competing interest

The authors declare that they have no known competing financial interests or personal relationships that could have appeared to influence the work reported in this paper.

Acknowledgment

Our gratitude goes to Katharina Pallitsch and Prof. Ernst Urban for recording 600 MHz and 500 MHz NMR spectra as well as to Daniel Dobusch for performing the HRMS measurements. We thank Prof. Thierry Langer for providing LigandScout. This work was supported by the Medical Imaging Cluster (MIC). We are grateful for the technical support of Thomas Zenz and Andreas Krcal.

References

[1] A.C. Kruse, B.K. Kobilka, D. Gautam, P.M. Sexton, A. Christopoulos, J. Wess, Muscarinic acetylcholine receptors: novel opportunities for drug development, Nat. Rev. Drug Discov. 13 (2014) 549–560. https://doi.org/10.1038/nrd4295.

[2] D. Dencker, M. Thomsen, G. Wörtwein, P. Weikop, Y. Cui, J. Jeon, J. Wess, A. Fink-Jensen, Muscarinic acetylcholine receptor subtypes as potential drug targets for the treatment of schizophrenia, drug abuse and Parkinson's disease, ACS Chem. Neurosci. 3 (2012) 80–89. https://doi.org/10.1021/cn200110q.

[3] P. Abrams, K.-E. Andersson, J.J. Buccafusco, C. Chapple, W.C. de Groat, A.D. Fryer, G. Kay, A. Laties, N.M. Nathanson, P.J. Pasricha, A.J. Wein, Muscarinic receptors: their distribution and function in body systems, and the implications for treating overactive bladder, Br. J. Pharmacol. 148 (2006) 565–578. https://doi.org/10.1038/sj.bjp.0706780.

[4] W.A.C. Burger, P.M. Sexton, A. Christopoulos, D.M. Thal, Toward an understanding of the structural basis of allostery in muscarinic acetylcholine receptors, J. Gen. Physiol. (2018) jgp.201711979. https://doi.org/10.1085/jgp.201711979.

[5] D.M. Thal, B. Sun, D. Feng, V. Nawaratne, K. Leach, C.C. Felder, M.G. Bures, D.A. Evans, W.I. Weis, P. Bachhawat, T.S. Kobilka, P.M. Sexton, B.K. Kobilka, A. Christopoulos, Crystal structures of the M1 and M4 muscarinic acetylcholine receptors, Nature. 531 (2016) 335–340. https://doi.org/10.1038/nature17188.

[6] P. Angeli, Trends in Receptor Research: Proceedings of the 8th Camerino-Noordwijkerhout Symposium, Camerino, Italy, 8-12 September 1991., Elsevier Science, Amsterdam, 2014. http://qut.eblib.com.au/patron/FullRecord.aspx?p=1837800 (accessed May 10, 2019).

[7] S.E. Yohn, P.J. Conn, Positive allosteric modulation of M 1 and M 4 muscarinic receptors as potential therapeutic treatments for schizophrenia, Neuropharmacology. 136 (2018) 438–448. https://doi.org/10.1016/j.neuropharm.2017.09.012.

[8] R.L. Papke, N.A. Horenstein, C. Stokes, Nicotinic activity of arecoline, the psychoactive element of “betel nuts”, suggests a basis for habitual use and anti-inflammatory activity, PLoS ONE. 10 (2015). https://doi.org/10.1371/journal.pone.0140907.

[9] G.Z. Dong, K. Kameyama, A. Rinken, T. Haga, Ligand binding properties of muscarinic acetylcholine receptor subtypes (m1-m5) expressed in baculovirus-infected insect cells., J. Pharmacol. Exp. Ther. 274 (1995) 378–384.

[10] W.C. Eckelman, Imaging of muscarinic receptors in the central nervous system, Curr. Pharm. Des. 12 (2006) 3901–3913.

[11] C.C. Felder, F.P. Bymaster, J. Ward, N. DeLapp, Therapeutic opportunities for muscarinic receptors in the central nervous system, J. Med. Chem. 43 (2000) 4333–4353. https://doi.org/10.1021/jm990607u.

[12] M. Wolf-Pflugmann, G. Lambrecht, J. Wess, E. Mutschler, Synthesis and muscarinic activity of a series of tertiary and quaternary N-substituted guvacine esters structurally related to arecoline and arecaidine propargyl ester, Arzneimittelforschung. 39 (1989) 539–544.

[13] S. Giri, J.R. Idle, C. Chen, T.M. Zabriskie, K.W. Krausz, F.J. Gonzalez, A metabolomic approach to the metabolism of the Areca nut alkaloids arecoline and aracaidine in the mouse, Chem. Res. Toxicol. 19 (2006) 818–827. https://doi.org/10.1021/tx0600402.

[14] R. Quirion, Cholinergic markers in Alzheimer disease and the autoregulation of acetylcholine release, J. Psychiatry Neurosci. JPN. 18 (1993) 226–234.

[15] W.C. Eckelman, M.R. Kilbourn, C.A. Mathis, Discussion of targeting proteins in vivo: in vitro guidelines, Nucl. Med. Biol. 33 (2006) 449–451. https://doi.org/10.1016/j.nucmedbio.2006.03.008.

[16] K.A. Frey, R.A. Koeppe, G.K. Mulholland, D. Jewett, R. Hichwa, R.L.E. Ehrenkaufer, J.E. Carey, D.M. Wieland, D.E. Kuhl, B.W. Agranoff, In vivo muscarinic cholingeric receptor imaging in human brain with [11C]scopolamine and positron emission tomography, J. Cereb. Blood Flow Metab. 12 (1992) 147–154. https://doi.org/10.1038/jcbfm.1992.18.

[17] S.L. Dewey, R.R. Macgregor, J.D. Brodie, B. Bendriem, P.T. King, N.D. Volkow, D.J. Schlyer, J.S. Fowler, A.P. Wolf, S.J. Gatley, R. Hitzemann, Mapping muscarinic receptors in human and baboon brain using [N-11C-methyl]-benztropine, Synapse. 5 (1990) 213–223. https://doi.org/10.1002/syn.890050307.

[18] K. Ridler, V. Cunningham, M. Huiban, L. Martarello, S. Pampols-Maso, J. Passchier, R.N. Gunn, G. Searle, A. Abi-Dargham, M. Slifstein, J. Watson, M. Laruelle, E.A. Rabiner, An evaluation of the brain distribution of [11 C]GSK1034702, a muscarinic-1 (M 1) positive allosteric modulator in the living human brain using positron emission tomography, EJNMMI Res. 4 (2014) 66. https://doi.org/10.1186/s13550-014-0066-y.

[19] J. Malmquist, K. Varnäs, M. Svedberg, F. Vallée, J.S. Albert, S.J. Finnema, M. Schou, Discovery of a novel muscarinic receptor PET radioligand with rapid kinetics in the monkey brain, ACS Chem. Neurosci. (2017). https://doi.org/10.1021/acschemneuro.7b00340.

[20] H.J.C. Buiter, J.E. Leysen, R.C. Schuit, A. Fisher, A.A. Lammertsma, A.D. Windhorst, Radiosynthesis and biological evaluation of the M1 muscarinic acetylcholine receptor agonist ligand [11C]AF150(S), J. Label. Compd. Radiopharm. 55 (2012) 264–273. https://doi.org/10.1002/jlcr.2932.
[21] P. Seeman, B. Madras, Imaging of the human brain in health and disease, Elsevier, 2013.
[22] X. Deng, A. Hatori, Z. Chen, K. Kumata, T. Shao, X. Zhang, T. Yamasaki, K. Hu, Q. Yu, L. Ma, G. Wang, L. Wang, Y. Shao, L. Josephson, S. Sun, M. Zhang, S. Liang, Synthesis and preliminary evaluation of ^{11}C-labeled VU0467485/AZ13713945 and its analogues for imaging muscarinic acetylcholine receptor subtype 4, ChemMedChem. 14 (2019) 303–309. https://doi.org/10.1002/cmdc.201800710.
[23] N.B. Nabulsi, D. Holden, M.-Q. Zheng, F. Bois, S.-F. Lin, S. Najafzadeh, H. Gao, J. Ropchan, T. Lara-Jaime, D. Labaree, A. Shirali, L. Slieker, C. Jesudason, V. Barth, A. Navarro, N. Kant, R.E. Carson, Y. Huang, Evaluation of ^{11}C-LSN3172176 as a novel PET tracer for imaging M_1 muscarinic acetylcholine receptors in nonhuman primates, J. Nucl. Med. 60 (2019) 1147–1153. https://doi.org/10.2967/jnumed.118.222034.
[24] G.C. Gullickson, D.E. Lewis, Synthesis of *N* -benzhydrylamides from nitriles by Ritter reactions in formic acid, Synthesis. (2003) 0681–0684. https://doi.org/10.1055/s-2003-38069.
[25] M.E. Kopach, U.K. Singh, M.E. Kobierski, W.G. Trankle, M.M. Murray, M.A. Pietz, M.B. Forst, G.A. Stephenson, V. Mancuso, T. Giard, M. Vanmarsenille, T. DeFrance, Practical synthesis of chiral 2-morpholine: (4-benzylmorpholin-2-(*S*)-yl)-(tetrahydropyran-4-yl)methanone mesylate, a useful pharmaceutical intermediate, Org. Process Res. Dev. 13 (2009) 209–224. https://doi.org/10.1021/op800247w.
[26] E.P. Lebois, C. Thorn, J.R. Edgerton, M. Popiolek, S. Xi, Muscarinic receptor subtype distribution in the central nervous system and relevance to aging and Alzheimer's disease, Neuropharmacology. 136 (2018) 362–373. https://doi.org/10.1016/j.neuropharm.2017.11.018.
[27] D.O. Kiesewetter, J. Lee, L. Lang, S.G. Park, C.H. Paik, W.C. Eckelman, Preparation of 18F-labeled muscarinic agonist with M2 selectivity, J. Med. Chem. 38 (1995) 5–8. https://doi.org/10.1021/jm00001a002.
[28] L. Ravasi, D.O. Kiesewetter, K. Shimoji, G. Lucignani, W.C. Eckelman, Why does the agonist [18F]FP-TZTP bind preferentially to the M2 muscarinic receptor?, Eur. J. Nucl. Med. Mol. Imaging. 33 (2006) 292–300. https://doi.org/10.1007/s00259-005-1966-x.
[29] J. Luo, S. Chen, S. Min, L. Peng, Reevaluation and update on efficacy and safety of neostigmine for reversal of neuromuscular blockade, Ther. Clin. Risk Manag. Volume 14 (2018) 2397–2406. https://doi.org/10.2147/TCRM.S179420.
[30] F.H. Darras, Y.-P. Pang, On the use of the experimentally determined enzyme inhibition constant as a measure of absolute binding affinity, BioRxiv. (2017). https://doi.org/10.1101/144204.
[31] C. Vraka, L. Nics, K.-H. Wagner, M. Hacker, W. Wadsak, M. Mitterhauser, Log P , a yesterday's value?, Nucl. Med. Biol. 50 (2017) 1–10. https://doi.org/10.1016/j.nucmedbio.2017.03.003.
[32] M.R. Kilbourn, P.J.H. Scott, Is logP truly dead?, Nucl. Med. Biol. 54 (2017) 41–42. https://doi.org/10.1016/j.nucmedbio.2017.08.006.
[33] C. Vraka, M. Mitterhauser, Reconsider logP!, Nucl. Med. Biol. 54 (2017) 42. https://doi.org/10.1016/j.nucmedbio.2017.08.007.
[34] H. Pajouhesh, G.R. Lenz, Medicinal chemical properties of successful central nervous system drugs, NeuroRX. 2 (2005) 541–553. https://doi.org/10.1602/neurorx.2.4.541.
[35] P. Champagne, J. Desroches, J.-F. Paquin, Organic fluorine as a hydrogen-bond acceptor: recent examples and applications, Synthesis. 47 (2014) 306–322. https://doi.org/10.1055/s-0034-1379537.
[36] H.H. Coenen, A.D. Gee, M. Adam, G. Antoni, C.S. Cutler, Y. Fujibayashi, J.M. Jeong, R.H. Mach, T.L. Mindt, V.W. Pike, A.D. Windhorst, Consensus nomenclature rules for radiopharmaceutical chemistry — Setting the record straight, Nucl. Med. Biol. 55 (2017) v–xi. https://doi.org/10.1016/j.nucmedbio.2017.09.004.

[37] European Directorate for the Quality of Medicines (EDQM), General Monograph 0125 - Radiopharmaceutical Preperations, in: Eur. Pharmacopoeia, Council of Europe, Strasbourg, 2016.
[38] D. Lodge, G.A.R. Johnston, D.R. Curtis, S.J. Brand, Effects of the Areca nut constituents arecaidine and guvacine on the action of GABA in the cat central nervous system, Brain Res. 136 (1977) 513–522. https://doi.org/10.1016/0006-8993(77)90075-0.
[39] C. Vraka, S. Mijailovic, V. Fröhlich, M. Zeilinger, E.-M. Klebermass, W. Wadsak, K.-H. Wagner, M. Hacker, M. Mitterhauser, Expanding LogP: Present possibilities, Nucl. Med. Biol. 58 (2018) 20–32. https://doi.org/10.1016/j.nucmedbio.2017.11.007.
[40] S. Göschl, H.P. Varbanov, S. Theiner, M.A. Jakupec, M. Galanski, B.K. Keppler, The role of the equatorial ligands for the redox behavior, mode of cellular accumulation and cytotoxicity of platinum(IV) prodrugs, J. Inorg. Biochem. 160 (2016) 264–274. https://doi.org/10.1016/j.jinorgbio.2016.03.005.
[41] G.C. Van de Bittner, E.L. Ricq, J.M. Hooker, A philosophy for CNS radiotracer design, Acc. Chem. Res. 47 (2014) 3127–3134. https://doi.org/10.1021/ar500233s.
[42] I.A.I. Ali, E.S.H.E. Ashry, R.R. Schmidt, Protection of hydroxy groups with diphenylmethyl and 9-fluorenyl trichloroacetimidates− effect on anomeric stereocontrol, Eur. J. Org. Chem. 2003 (2003) 4121–4131. https://doi.org/10.1002/ejoc.200300323.
[43] M. Pawlicki, L. Latos-Grażyński, L. Szterenberg, 5,10,15-Triaryl-21,23-dioxacorrole and its isomer with a protruding furan ring, J. Org. Chem. 67 (2002) 5644–5653. https://doi.org/10.1021/jo025773f.
[44] S. Song, S.-F. Zhu, L.-Y. Pu, Q.-L. Zhou, Iridium-catalyzed enantioselective hydrogenation of unsaturated heterocyclic acids, Angew. Chem. 125 (2013) 6188–6191. https://doi.org/10.1002/ange.201301341.
[45] J.B. Baell, G.A. Holloway, New substructure filters for removal of pan assay interference Compounds (PAINS) from screening libraries and for their exclusion in bioassays, J. Med. Chem. 53 (2010) 2719–2740. https://doi.org/10.1021/jm901137j.
[46] ICH Harmonised Tripartite Guideline: Validation of Analytical Procedures: Text and Methodology Q2(R1), (1996).
[47] C. Rami-Mark, N. Berroterán-Infante, C. Philippe, S. Foltin, C. Vraka, A. Hoepping, R. Lanzenberger, M. Hacker, M. Mitterhauser, W. Wadsak, Radiosynthesis and first preclinical evaluation of the novel norepinephrine transporter pet-ligand [11C]ME@HAPTHI, EJNMMI Res. 5 (2015) 34. https://doi.org/10.1186/s13550-015-0113-3.
[48] K.N. Klotz, J. Hessling, J. Hegler, C. Owman, B. Kull, B.B. Fredholm, M.J. Lohse, Comparative pharmacology of human adenosine receptor subtypes - characterization of stably transfected receptors in CHO cells, Naunyn. Schmiedebergs Arch. Pharmacol. 357 (1998) 1–9.
[49] A. Kumar, T. Darreh-Shori, DMSO: A mixed-competitive inhibitor of human acetylcholinesterase, ACS Chem. Neurosci. 8 (2017) 2618–2625. https://doi.org/10.1021/acschemneuro.7b00344.
[50] P. Valuskova, V. Farar, S. Forczek, I. Krizova, J. Myslivecek, Autoradiography of 3H-pirenzepine and 3H-AFDX-384 in mouse brain regions: possible insights into M1, M2, and M4 muscarinic receptors distribution, Front. Pharmacol. 9 (2018) 124. https://doi.org/10.3389/fphar.2018.00124.

Highlights

- Fifteen novel arecoline derivatives synthesized
- Benzhydryl esters are high affinity ligands for muscarinic acetylcholine receptors
- Pronounced subtype selectivity for M1
- Straightforward carbon-11 labeling

Declaration of interests

☒ The authors declare that they have no known competing financial interests or personal relationships that could have appeared to influence the work reported in this paper.

☐The authors declare the following financial interests/personal relationships which may be considered as potential competing interests: